

UNITED STATES AIR FORCE
SUMMER RESEARCH PROGRAM -- 1998
GRADUATE STUDENT RESEARCH PROGRAM FINAL REPORTS

VOLUME 9

ROME LABORATORY

RESEARCH & DEVELOPMENT LABORATORIES
5800 Uplander Way
Culver City, CA 90230-6608

Program Director, RDL Program Manager, AFOSR
Gary Moore Colonel Jan Cerveny

Program Manager, RDL Program Administrator, RDL
Scott Licoscos Johnetta Thompson

Program Administrator, RDL
Rebecca Kelly-Clemmons

Submitted to:

AIR FORCE OFFICE OF SCIENTIFIC RESEARCH
Bolling Air Force Base
Washington, D.C.

20010319
041

December 1998

AQM01-06-1213

PREFACE

Reports in this volume are numbered consecutively beginning with number 1. Each report is paginated with the report number followed by consecutive page numbers, e.g., 1-1, 1-2, 1-3; 2-1, 2-2, 2-3.

This document is one of a set of 15 volumes describing the 1998 AFOSR Summer Research Program. The following volumes comprise the set:

<u>VOLUME</u>	<u>TITLE</u>
1	Program Management Report
<i>Summer Faculty Research Program (SFRP) Reports</i>	
2	Armstrong Laboratory
3	Phillips Laboratory
4	Rome Laboratory
5A & 5B	Wright Laboratory
6	Arnold Engineering Development Center, Air Logistics Centers, United States Air Force Academy and Wilford Hall Medical Center
<i>Graduate Student Research Program (GSRP) Reports</i>	
7	Armstrong Laboratory
8	Phillips Laboratory
9	Rome Laboratory
10	Wright Laboratory
11	Arnold Engineering Development Center, and Wilford Hall Medical Center
<i>High School Apprenticeship Program (HSAP) Reports</i>	
12	Armstrong Laboratory
13	Phillips Laboratory
14	Rome Laboratory
15A, 15B & 15C	Wright Laboratory

REPORT DOCUMENTATION PAGE

Public reporting burden for this collection of information is estimated to average 1 hour per response, including the time for reviewing instructions, the collection of information. Send comments regarding this burden estimate or any other aspect of this collection of information, including Operations and Reports, 1215 Jefferson Davis Highway, Suite 1204, Arlington, VA 22202-4302, and to the Office of Management and Budget.

g and reviewing
for Information

AFRL-SR-BL-TR-00-

0785

1. AGENCY USE ONLY (Leave blank)	2. REPORT DATE	3. R	
	December, 1998		
4. TITLE AND SUBTITLE 1998 Summer Research Program (SRP), Graduate Student Research Program (GSRP), Final Reports, Volume 9, Rome Laboratory		5. FUNDING NUMBERS F49620-93-C-0063	
6. AUTHOR(S) Gary Moore			
7. PERFORMING ORGANIZATION NAME(S) AND ADDRESS(ES) Research & Development Laboratories (RDL) 5800 Uplander Way Culver City, CA 90230-6608		8. PERFORMING ORGANIZATION REPORT NUMBER	
9. SPONSORING/MONITORING AGENCY NAME(S) AND ADDRESS(ES) Air Force Office of Scientific Research (AFOSR) 801 N. Randolph St. Arlington, VA 22203-1977		10. SPONSORING/MONITORING AGENCY REPORT NUMBER	
11. SUPPLEMENTARY NOTES			
12a. DISTRIBUTION AVAILABILITY STATEMENT Approved for Public Release		12b. DISTRIBUTION CODE	
13. ABSTRACT (Maximum 200 words) The United States Air Force Summer Research Program (USAF-SRP) is designed to introduce university, college, and technical institute faculty members, graduate students, and high school students to Air Force research. This is accomplished by the faculty members (Summer Faculty Research Program, (SFRP)), graduate students (Graduate Student Research Program (GSRP)), and high school students (High School Apprenticeship Program (HSAP)) being selected on a nationally advertised competitive basis during the summer intersession period to perform research at Air Force Research Laboratory (AFRL) Technical Directorates, Air Force Air Logistics Centers (ALC), and other AF Laboratories. This volume consists of a program overview, program management statistics, and the final technical reports from the GSRP participants at the Rome Laboratory.			
14. SUBJECT TERMS Air Force Research, Air Force, Engineering, Laboratories, Reports, Summer, Universities, Faculty, Graduate Student, High School Student		15. NUMBER OF PAGES	
		16. PRICE CODE	
17. SECURITY CLASSIFICATION OF REPORT Unclassified	18. SECURITY CLASSIFICATION OF THIS PAGE Unclassified	19. SECURITY CLASSIFICATION OF ABSTRACT Unclassified	20. LIMITATION OF ABSTRACT UL

GENERAL INSTRUCTIONS FOR COMPLETING SF 298

The Report Documentation Page (RDP) is used in announcing and cataloging reports. It is important that this information be consistent with the rest of the report, particularly the cover and title page. Instructions for filling in each block of the form follow. It is important to *stay within the lines* to meet *optical scanning requirements*.

Block 1. Agency Use Only (Leave blank).

Block 2. Report Date. Full publication date including day, month, and year, if available (e.g. 1 Jan 88). Must cite at least the year.

Block 3. Type of Report and Dates Covered. State whether report is interim, final, etc. If applicable, enter inclusive report dates (e.g. 10 Jun 87 - 30 Jun 88).

Block 4. Title and Subtitle. A title is taken from the part of the report that provides the most meaningful and complete information. When a report is prepared in more than one volume, repeat the primary title, add volume number, and include subtitle for the specific volume. On classified documents enter the title classification in parentheses.

Block 5. Funding Numbers. To include contract and grant numbers; may include program element number(s), project number(s), task number(s), and work unit number(s). Use the following labels:

C - Contract
G - Grant
PE - Program Element

PR - Project
TA - Task
WU - Work Unit
Accession No.

Block 6. Author(s). Name(s) of person(s) responsible for writing the report, performing the research, or credited with the content of the report. If editor or compiler, this should follow the name(s).

Block 7. Performing Organization Name(s) and Address(es). Self-explanatory.

Block 8. Performing Organization Report Number. Enter the unique alphanumeric report number(s) assigned by the organization performing the report.

Block 9. Sponsoring/Monitoring Agency Name(s) and Address(es). Self-explanatory.

Block 10. Sponsoring/Monitoring Agency Report Number. //f known)

Block 11. Supplementary Notes. Enter information not included elsewhere such as: Prepared in cooperation with....; Trans. of....; To be published in.... When a report is revised, include a statement whether the new report supersedes or supplements the older report.

Block 12a. Distribution/Availability Statement. Denotes public availability or limitations. Cite any availability to the public. Enter additional limitations or special markings in all capitals (e.g. NOFORN, REL, ITAR).

DOD - See DoDD 5230.24, "Distribution Statements on Technical Documents."
DOE - See authorities.
NASA - See Handbook NHB 2200.2.
NTIS - Leave blank.

Block 12b. Distribution Code.

DOD - Leave blank.
DOE - Enter DOE distribution categories from the Standard Distribution for Unclassified Scientific and Technical Reports.
Leave blank.
NASA - Leave blank.
NTIS -

Block 13. Abstract. Include a brief (*Maximum 200 words*) factual summary of the most significant information contained in the report.

Block 14. Subject Terms. Keywords or phrases identifying major subjects in the report.

Block 15. Number of Pages. Enter the total number of pages.

Block 16. Price Code. Enter appropriate price code (*NTIS only*).

Blocks 17. - 19. Security Classifications. Self-explanatory. Enter U.S. Security Classification in accordance with U.S. Security Regulations (i.e., UNCLASSIFIED). If form contains classified information, stamp classification on the top and bottom of the page.

Block 20. Limitation of Abstract. This block must be completed to assign a limitation to the abstract. Enter either UL (unlimited) or SAR (same as report). An entry in this block is necessary if the abstract is to be limited. If blank, the abstract is assumed to be unlimited.

GSRP FINAL REPORT TABLE OF CONTENTS**i-vi**

1. INTRODUCTION	1
2. PARTICIPATION IN THE SUMMER RESEARCH PROGRAM	2
3. RECRUITING AND SELECTION	3
4. SITE VISITS	4
5. HBCU/MI PARTICIPATION	4
6. SRP FUNDING SOURCES	5
7. COMPENSATION FOR PARTICIPATIONS	5
8. CONTENTS OF THE 1995 REPORT	6

APPENDICIES:

A. PROGRAM STATISTICAL SUMMARY	A-1
B. SRP EVALUATION RESPONSES	B-1

GSRP FINAL REPORTS

SRP Final Report Table of Contents

<u>Author</u>	<u>University/Institution Report Title</u>	<u>Armstrong Laboratory Directorate</u>	<u>Vol-Page</u>
MR Jason M Henry	Ohio University , Athens , OH Phantom/Merlin Force-Reflecting Teleoperation:Implementation	AFRL/HEC _____	7- 1
MR Keith S Jones	University of Cincinnati , Cincinnati , OH Issues in Steady-State Visual Evoked Response Based Control	AFRL/HEC _____	7- 2
MR Christian A Kijora	Arizona State University , Mesa , AZ Research Techniques A Search for Crew Resource Management Documents	AFRL/HEA _____	7- 3
MS Vanessa D Le	Univ of Texas at Austin , Austin , TX Permeability Characteristics of an Endothelial Cell Model of the Blood-Brain barrier	AFRL/HED _____	7- 4
MR Peter D Naegele	University of Toledo , Toledo , OH Anisotropies in Visual Search Performance Across The Upper and Lower Visual Fields as a Function of	AFRL/HEP _____	7- 5
MS Nicole L Proulx	University of Dayton , Dayton , OH Nefotiation at a Distance: Why you Might want to use the Telephone	AFRL/HES _____	7- 6
MS Mary K Sheehan	Texas A & M Univ-College Station , College Station , TX Understanding Disagreement Across Rating Sources An Assessment of the Measurement Equivalence of Rat	AFRL/HEJ _____	7- 7
MR Brian D Simpson	Wright State University , Dayton , OH The Effect of Spatial Separation and Onset Asynchrony on the Detectability and Intelligibility of a	AFRL/HES _____	7- 8
MS Julie A Stiles-Shipley	Bowling Green State University , Bowling Green , OH The Rate of Skill Acquisition for males and females on space Frotress	AFRL/HEJ _____	7- 9
MR Michael E Stiso	University of Oregon , Eugene , OR Weighing The Importance of Spatial Organization and Priority of Targets on UAV Mission Planning Whic	AFRL/HEJ _____	7- 10

SRP Final Report Table of Contents

<u>Author</u>	<u>University/Institution Report Title</u>	<u>Phillips Laboratory Directorate</u>	<u>Vol-Page</u>
MR Benjamin J Bernocco	Pennsylvania State University , University Park , PA A study of Optimal finite-Thrust SpaceCraft Trajectories for the Techsat 21 Mission	AFRL/VSS	8- 1
MR Robert J Fuentes	Univ of Colorado at Boulder , Boulder , CO Stable Controller Design For Deployable Precision Structures Using Perturbation Theory	AFRL/VSD	8- 2
MR Jeffery M Ganley	University of New Mexico , Albuquerque , NM Determination of the Residual Stress Profile in a thin Composite Part	AFRL/VSD	8- 3
MR David A Joiner	Rensselaer Polytechnic Instit , Troy , NY A Study of the Effects of Novae on The Infrared Celestial Background	AFRL/VSB	8- 4
MS Johnelle L Korieth	Univ of Texas at Dallas , Richardson , TX A Computational Analysis of Stacked Blumleins Used in Pulsed Power Devices	AFRL/DEH	8- 5
MS Elizabeth M Monaco	Holy Cross College , Worcester , MA Approximating Morse Potentials Numerically and Analytically	AFRL/VSB	8- 6
MR Tyrone A Ospino	University of Puerto Rico , San Juan , PR Conducting fluid Real-Time 2-D Electronic Interpolator and Spatial Filter For wavefront Sensor-To-Co	AFRL/DEB	8- 7
MR Kenneth F Stephens II	University of North Texas , Denton , TX Simulation of Plasma-Wall mixing in a Magnetized Target Fusion Concept	AFRL/DEH	8- 8
MR Michael V Wood	Pennsylvania State University , University Park , PA Characterization of Spatial Light Modulator for Aberration compensation of Severely Distorted Primary	AFRL/DEB	8- 9

SRP Final Report Table of Contents

Author	University/Institution Report Title	Rome Laboratory Directorate	Vol-Page
MR Sang H Bae	Univ of Calif, Los Angeles , Los Angeles , CA A Simulation Study of the Vulnerabilities in Commercial Satellite Constellations	AFRL/IFG	9- 1
MR Keith R Buck	Colorado State University , Fort Collins , CO Near-Optimal Routing of Unmanned Surveillance Platforms	AFRL/IFE	9- 2
MR Kevin P Crossway	SUNY OF Tech Utica , Utica , NY	AFRL/IFT	9- 3
MR Brian R Waterhouse	Syracuse University , Syracuse , NY Empirical and Theoretical Foundations for a Two-Dimensional Non-Homogeneity Detector for Radar	AFRL/SNR	9- 4

SRP Final Report Table of Contents

Author	University/Institution Report Title	Wright Laboratory Directorate	Vol-Page
MR Jeffrey C Anderson	Clemson University , Clemson , SC Growth and Characterization of 3-inch Nitride Semiconducting Epitaxial Films	AFRL/SNH	10- 1
MR Erik L Antonson	Northern Illinois University , Urbana , IL Modified herriott Cell Interferometr for Pulsed Plasma Thruster Neutral Density Measurements	AFRL/PRR	10- 2
MR Daniel J Bodony	Purdue University , West Lafayette , IN MDICE Analysis of An F-18C Wing	AFRL/VAA	10- 3
MR Gregory C Harding	Florida Inst of Technology/Geo. Washingt , Melbourne , FL Interactions between Weakly Ionized Gas Plasmas and Shock Waves A Revoew	AFRL/PRT	10- 4
MR John L Hazel	Western Michigan University , Kalamazoo , MI The Physical Basis of Boid And Crotaline Infrared Detection	AFRL/MLP	10- 5
MR Timothy J Leger	Wright State University , Dayton , OH Enhancements to a Direct Aeroelastic Stability Computational Model	AFRL/VAS	10- 6
MR Ronald O Nelson	University of Idaho , Moscow , ID A Detailed Study of the Numerical properties of FDTD Algorithms for Dispersive Media	AFRL/VAA	10- 7
MR Andrew D Panetta	Rensselaer Polytechnic Instit , Troy , NY The Design of a Double Strut Support System for Low Speed wind Tunnel Testing of Rotating, Axisymmet	AFRL/PRS	10- 8
MR Eduardo L Pasiliao	University of Florida , Gainesville , FL A Greedy Randomized Adaptive Search Procedure for the Multi-Criteria Radio Link Frequency Assignment	AFRL/MN	10- 9
MR Craig A Riviello	Wright State University , Dayton , OH In-SituSynthesis of Discontinuously Reinforced Titanium alloy Composites Via Blended Eldelemental Powd	AFRL/ML	10- 10
MS Lisa A Schaefer	Arizona State University . Tempe , AZ Evaluation of Using Agents for Factory Layout Affordability	AFRL/ML	10- 11

SRP Final Report Table of Contents

Author	University/Institution Report Title	Wright Laboratory Directorate	Vol-Page
MS Katherine J Schafer	University of Detroit , Detroit , MI Synthesis of 7-Benzothiazol-2YL-9,9-Didecylfluorene-2Ylamine: A Versatile Intermediate For a New Ser	AFRL/ML	10- 12
MR Aboubakar Traore	Stevens Inst of Technology , Hoboken , NJ Theory of Envelope-Function within 6*6 Luttinger Model in holes Subband States of Si Ge Quantum Well	AFRL/SNH	10- 13
MR Robert A Weisenseel	Boston University , Boston , MA MRF Segmentation for Feature Extraction in Sar Chip Classification	AFRL/SNA	10- 14
MR Jerry M Wohletz	Massachusetts Inst of Technology , Cambridge , MA Parameter Estimation for the Tailless Advanced Fighter Aircraft (TAFA)	AFRL/VAC	10- 15

SRP Final Report Table of Contents

Author	University/Institution Report Title	Arnold Engineering Development Center Directorate	Vol-Page
MR Gregory M Laskowski	Stanford University , Stanford , CA Wind Validation: Incompressible Turbulent Flow Past A Flat Plate	AEDC	11- 1
MS Donna M Lehman	Univ of Texas Health Science Center , San Antonio , TX Relationship Between Growth Hormone and Myelin Basic Protein Expression In Vivo	WHMC	11- 2

1. INTRODUCTION

The Summer Research Program (SRP), sponsored by the Air Force Office of Scientific Research (AFOSR), offers paid opportunities for university faculty, graduate students, and high school students to conduct research in U.S. Air Force research laboratories nationwide during the summer.

Introduced by AFOSR in 1978, this innovative program is based on the concept of teaming academic researchers with Air Force scientists in the same disciplines using laboratory facilities and equipment not often available at associates' institutions.

The Summer Faculty Research Program (SFRP) is open annually to approximately 150 faculty members with at least two years of teaching and/or research experience in accredited U.S. colleges, universities, or technical institutions. SFRP associates must be either U.S. citizens or permanent residents.

The Graduate Student Research Program (GSRP) is open annually to approximately 100 graduate students holding a bachelor's or a master's degree; GSRP associates must be U.S. citizens enrolled full time at an accredited institution.

The High School Apprentice Program (HSAP) annually selects about 125 high school students located within a twenty mile commuting distance of participating Air Force laboratories.

AFOSR also offers its research associates an opportunity, under the Summer Research Extension Program (SREP), to continue their AFOSR-sponsored research at their home institutions through the award of research grants. In 1994 the maximum amount of each grant was increased from \$20,000 to \$25,000, and the number of AFOSR-sponsored grants decreased from 75 to 60. A separate annual report is compiled on the SREP.

The numbers of projected summer research participants in each of the three categories and SREP "grants" are usually increased through direct sponsorship by participating laboratories.

AFOSR's SRP has well served its objectives of building critical links between Air Force research laboratories and the academic community, opening avenues of communications and forging new research relationships between Air Force and academic technical experts in areas of national interest, and strengthening the nation's efforts to sustain careers in science and engineering. The success of the SRP can be gauged from its growth from inception (see Table 1) and from the favorable responses the 1997 participants expressed in end-of-tour SRP evaluations (Appendix B).

AFOSR contracts for administration of the SRP by civilian contractors. The contract was first awarded to Research & Development Laboratories (RDL) in September 1990. After completion of the 1990 contract, RDL (in 1993) won the recompetition for the basic year and four 1-year options.

2. PARTICIPATION IN THE SUMMER RESEARCH PROGRAM

The SRP began with faculty associates in 1979; graduate students were added in 1982 and high school students in 1986. The following table shows the number of associates in the program each year.

YEAR	SRP Participation, by Year			TOTAL
	SFRP	GSRP	HSAP	
1979	70			70
1980	87			87
1981	87			87
1982	91	17		108
1983	101	53		154
1984	152	84		236
1985	154	92		246
1986	158	100	42	300
1987	159	101	73	333
1988	153	107	101	361
1989	168	102	103	373
1990	165	121	132	418
1991	170	142	132	444
1992	185	121	159	464
1993	187	117	136	440
1994	192	117	133	442
1995	190	115	137	442
1996	188	109	138	435
1997	148	98	140	427
1998	85	40	88	213

Beginning in 1993, due to budget cuts, some of the laboratories weren't able to afford to fund as many associates as in previous years. Since then, the number of funded positions has remained fairly constant at a slightly lower level.

3. RECRUITING AND SELECTION

The SRP is conducted on a nationally advertised and competitive-selection basis. The advertising for faculty and graduate students consisted primarily of the mailing of 8,000 52-page SRP brochures to chairpersons of departments relevant to AFOSR research and to administrators of grants in accredited universities, colleges, and technical institutions. Historically Black Colleges and Universities (HBCUs) and Minority Institutions (MIs) were included. Brochures also went to all participating USAF laboratories, the previous year's participants, and numerous individual requesters (over 1000 annually).

RDL placed advertisements in the following publications: *Black Issues in Higher Education*, *Winds of Change*, and *IEEE Spectrum*. Because no participants list either *Physics Today* or *Chemical & Engineering News* as being their source of learning about the program for the past several years, advertisements in these magazines were dropped, and the funds were used to cover increases in brochure printing costs.

High school applicants can participate only in laboratories located no more than 20 miles from their residence. Tailored brochures on the HSAP were sent to the head counselors of 180 high schools in the vicinity of participating laboratories, with instructions for publicizing the program in their schools. High school students selected to serve at Wright Laboratory's Armament Directorate (Eglin Air Force Base, Florida) serve eleven weeks as opposed to the eight weeks normally worked by high school students at all other participating laboratories.

Each SFRP or GSRP applicant is given a first, second, and third choice of laboratory. High school students who have more than one laboratory or directorate near their homes are also given first, second, and third choices.

Laboratories make their selections and prioritize their nominees. AFOSR then determines the number to be funded at each laboratory and approves laboratories' selections.

Subsequently, laboratories use their own funds to sponsor additional candidates. Some selectees do not accept the appointment, so alternate candidates are chosen. This multi-step selection procedure results in some candidates being notified of their acceptance after scheduled deadlines. The total applicants and participants for 1998 are shown in this table.

1998 Applicants and Participants			
PARTICIPANT CATEGORY	TOTAL APPLICANTS	SELECTEES	DECLINING SELECTEES
SFRP	382	85	13
(HBCU/MI)	(0)	(0)	(0)
GSRP	130	40	7
(HBCU/MI)	(0)	(0)	(0)
HSAP	328	88	22
TOTAL	840	213	42

4. SITE VISITS

During June and July of 1998, representatives of both AFOSR/NI and RDL visited each participating laboratory to provide briefings, answer questions, and resolve problems for both laboratory personnel and participants. The objective was to ensure that the SRP would be as constructive as possible for all participants. Both SRP participants and RDL representatives found these visits beneficial. At many of the laboratories, this was the only opportunity for all participants to meet at one time to share their experiences and exchange ideas.

5. HISTORICALLY BLACK COLLEGES AND UNIVERSITIES AND MINORITY INSTITUTIONS (HBCU/MIs)

Before 1993, an RDL program representative visited from seven to ten different HBCU/MIs annually to promote interest in the SRP among the faculty and graduate students. These efforts were marginally effective, yielding a doubling of HBCI/MI applicants. In an effort to achieve AFOSR's goal of 10% of all applicants and selectees being HBCU/MI qualified, the RDL team decided to try other avenues of approach to increase the number of qualified applicants. Through the combined efforts of the AFOSR Program Office at Bolling AFB and RDL, two very active minority groups were found, HACU (Hispanic American Colleges and Universities) and AISES (American Indian Science and Engineering Society). RDL is in communication with representatives of each of these organizations on a monthly basis to keep up with their activities and special events. Both organizations have widely-distributed magazines/quarterlies in which RDL placed ads.

Since 1994 the number of both SFRP and GSRP HBCU/MI applicants and participants has increased ten-fold, from about two dozen SFRP applicants and a half dozen selectees to over 100 applicants and two dozen selectees, and a half-dozen GSRP applicants and two or three selectees to 18 applicants and 7 or 8 selectees. Since 1993, the SFRP had a two-fold applicant increase and a two-fold selectee increase. Since 1993, the GSRP had a three-fold applicant increase and a three to four-fold increase in selectees.

In addition to RDL's special recruiting efforts, AFOSR attempts each year to obtain additional funding or use leftover funding from cancellations the past year to fund HBCU/MI associates.

YEAR	SFRP		GSRP	
	Applicants	Participants	Applicants	Participants
1985	76	23	15	11
1986	70	18	20	10
1987	82	32	32	10
1988	53	17	23	14
1989	39	15	13	4
1990	43	14	17	3
1991	42	13	8	5
1992	70	13	9	5
1993	60	13	6	2
1994	90	16	11	6
1995	90	21	20	8
1996	119	27	18	7

6. SRP FUNDING SOURCES

Funding sources for the 1998 SRP were the AFOSR-provided slots for the basic contract and laboratory funds. Funding sources by category for the 1998 SRP selected participants are shown here.

1998 SRP FUNDING CATEGORY	SFRP	GSRP	HSAP
AFOSR Basic Allocation Funds	67	38	75
USAF Laboratory Funds	17	2	13
Slots Added by AFOSR (Leftover Funds)	0	0	0
HBCU/MI By AFOSR (Using Procured Addn'l Funds)	0	0	N/A
TOTAL	84	40	88

7. COMPENSATION FOR PARTICIPANTS

Compensation for SRP participants, per five-day work week, is shown in this table.

1998 SRP Associate Compensation

PARTICIPANT CATEGORY	1991	1992	1993	1994	1995	1996	1997	1998
Faculty Members	\$690	\$718	\$740	\$740	\$740	\$770	\$770	\$793
Graduate Student (Master's Degree)	\$425	\$442	\$455	\$455	\$455	\$470	\$470	\$484
Graduate Student (Bachelor's Degree)	\$365	\$380	\$391	\$391	\$391	\$400	\$400	\$412
High School Student (First Year)	\$200	\$200	\$200	\$200	\$200	\$200	\$200	\$200
High School Student (Subsequent Years)	\$240	\$240	\$240	\$240	\$240	\$240	\$240	\$240

The program also offered associates whose homes were more than 50 miles from the laboratory an expense allowance (seven days per week) of \$52/day for faculty and \$41/day for graduate students. Transportation to the laboratory at the beginning of their tour and back to their home destinations at the end was also reimbursed for these participants. Of the combined SFRP and GSRP associates, 65 % claimed travel reimbursements at an average round-trip cost of \$730.

Faculty members were encouraged to visit their laboratories before their summer tour began. All costs of these orientation visits were reimbursed. Forty-three percent (85 out of 188) of faculty associates took orientation trips at an average cost of \$449. By contrast, in 1993, 58 % of SFRP associates elected to take an orientation visits at an average cost of \$685; that was the highest

percentage of associates opting to take an orientation trip since RDL has administered the SRP, and the highest average cost of an orientation trip.

Program participants submitted biweekly vouchers countersigned by their laboratory research focal point, and RDL issued paychecks so as to arrive in associates' hands two weeks later.

This is the third year of using direct deposit for the SFRP and GSRP associates. The process went much more smoothly with respect to obtaining required information from the associates, about 15% of the associates' information needed clarification in order for direct deposit to properly function as opposed to 7% from last year. The remaining associates received their stipend and expense payments via checks sent in the US mail.

HSAP program participants were considered actual RDL employees, and their respective state and federal income tax and Social Security were withheld from their paychecks. By the nature of their independent research, SFRP and GSRP program participants were considered to be consultants or independent contractors. As such, SFRP and GSRP associates were responsible for their own income taxes, Social Security, and insurance.

8. CONTENTS OF THE 1998 REPORT

The complete set of reports for the 1998 SRP includes this program management report (Volume 1) augmented by fifteen volumes of final research reports by the 1998 associates, as indicated below:

1998 SRP Final Report Volume Assignments

LABORATORY	SFRP	GSRP	HSAP
Armstrong	2	7	12
Phillips	3	8	13
Rome	4	9	14
Wright	5A, 5B	10	15
AEDC, ALCs, USAFA, WHMC	6	11	

APPENDIX A -- PROGRAM STATISTICAL SUMMARY

A. Colleges/Universities Represented

Selected SFRP associates represented 169 different colleges, universities, and institutions, GSRP associates represented 95 different colleges, universities, and institutions.

B. States Represented

SFRP -Applicants came from 47 states plus Washington D.C. Selectees represent 44 states.

GSRP - Applicants came from 44 states. Selectees represent 32 states.

HSAP - Applicants came from thirteen states. Selectees represent nine states.

Total Number of Participants	
SFRP	85
GSRP	40
HSAP	88
TOTAL	213

Degrees Represented			
	SFRP	GSRP	TOTAL
Doctoral	83	0	83
Master's	1	3	4
Bachelor's	0	22	22
TOTAL	186	25	109

SFRP Academic Titles	
Assistant Professor	36
Associate Professor	34
Professor	15
Instructor	0
Chairman	0
Visiting Professor	0
Visiting Assoc. Prof.	0
Research Associate	0
TOTAL	85

Source of Learning About the SRP		
Category	Applicants	Selectees
Applied/participated in prior years	177	47
Colleague familiar with SRP	104	24
Brochure mailed to institution	101	21
Contact with Air Force laboratory	101	39
<i>IEEE Spectrum</i>	12	1
<i>BIIHE</i>	4	0
Other source	117	30
TOTAL	616	162

APPENDIX B – SRP EVALUATION RESPONSES

1. OVERVIEW

Evaluations were completed and returned to RDL by four groups at the completion of the SRP. The number of respondents in each group is shown below.

Table B-1. Total SRP Evaluations Received

Evaluation Group	Responses
SFRP & GSRPs	100
HSAPs	75
USAF Laboratory Focal Points	84
USAF Laboratory HSAP Mentors	6

All groups indicate unanimous enthusiasm for the SRP experience.

The summarized recommendations for program improvement from both associates and laboratory personnel are listed below:

- A. Better preparation on the labs' part prior to associates' arrival (i.e., office space, computer assets, clearly defined scope of work).
- B. Faculty Associates suggest higher stipends for SFRP associates.
- C. Both HSAP Air Force laboratory mentors and associates would like the summer tour extended from the current 8 weeks to either 10 or 11 weeks; the groups state it takes 4-6 weeks just to get high school students up-to-speed on what's going on at laboratory. (Note: this same argument was used to raise the faculty and graduate student participation time a few years ago.)

2. 1998 USAF LABORATORY FOCAL POINT (LFP) EVALUATION RESPONSES

The summarized results listed below are from the 84 LFP evaluations received.

1. LFP evaluations received and associate preferences:

Table B-2. Air Force LFP Evaluation Responses (By Type)

Lab	Evals Recv'd	How Many Associates Would You Prefer To Get ?				(% Response)			
		SFRP				GSRP (w/Univ Professor)			
		0	1	2	3+	0	1	2	3+
AEDC	0	-	-	-	-	-	-	-	-
WHMC	0	-	-	-	-	-	-	-	-
AL	7	28	28	28	14	54	14	28	0
USAFA	1	0	100	0	0	100	0	0	0
PL	25	40	40	16	4	88	12	0	0
RL	5	60	40	0	0	80	10	0	0
WL	46	30	43	20	6	78	17	4	0
Total	84	32%	50%	13%	5%	80%	11%	6%	0%
								73%	23%
								4%	0%

LFP Evaluation Summary. The summarized responses, by laboratory, are listed on the following page. LFPs were asked to rate the following questions on a scale from 1 (below average) to 5 (above average).

2. LFPs involved in SRP associate application evaluation process:

- a. Time available for evaluation of applications:
- b. Adequacy of applications for selection process:

3. Value of orientation trips:

4. Length of research tour:

- 5 a. Benefits of associate's work to laboratory:
b. Benefits of associate's work to Air Force:
- 6 a. Enhancement of research qualifications for LFP and staff:
b. Enhancement of research qualifications for SFRP associate:
c. Enhancement of research qualifications for GSRP associate:
- 7 a. Enhancement of knowledge for LFP and staff:
b. Enhancement of knowledge for SFRP associate:
c. Enhancement of knowledge for GSRP associate:

8. Value of Air Force and university links:

9. Potential for future collaboration:

- 10. a. Your working relationship with SFRP:
b. Your working relationship with GSRP:

11. Expenditure of your time worthwhile:

(Continued on next page)

12. Quality of program literature for associate:
 13. a. Quality of RDL's communications with you:
 b. Quality of RDL's communications with associates:
 14. Overall assessment of SRP:

Table B-3. Laboratory Focal Point Responses to above questions

	<i>AEDC</i>	<i>AL</i>	<i>USAF</i>	<i>PL</i>	<i>RL</i>	<i>WHMC</i>	<i>WL</i>
<i># Evals Recv'd</i>	0	7	1	14	5	0	46
<i>Question #</i>	<i>A</i>						
2	-	86 %	0 %	88 %	80 %	-	85 %
2a	-	4.3	n/a	3.8	4.0	-	3.6
2b	-	4.0	n/a	3.9	4.5	-	4.1
3	-	4.5	n/a	4.3	4.3	-	3.7
4	-	4.1	4.0	4.1	4.2	-	3.9
5a	-	4.3	5.0	4.3	4.6	-	4.4
5b	-	4.5	n/a	4.2	4.6	-	4.3
6a	-	4.5	5.0	4.0	4.4	-	4.3
6b	-	4.3	n/a	4.1	5.0	-	4.4
6c	-	3.7	5.0	3.5	5.0	-	4.3
7a	-	4.7	5.0	4.0	4.4	-	4.3
7b	-	4.3	n/a	4.2	5.0	-	4.4
7c	-	4.0	5.0	3.9	5.0	-	4.3
8	-	4.6	4.0	4.5	4.6	-	4.3
9	-	4.9	5.0	4.4	4.8	-	4.2
10a	-	5.0	n/a	4.6	4.6	-	4.6
10b	-	4.7	5.0	3.9	5.0	-	4.4
11	-	4.6	5.0	4.4	4.8	-	4.4
12	-	4.0	4.0	4.0	4.2	-	3.8
13a	-	3.2	4.0	3.5	3.8	-	3.4
13b	-	3.4	4.0	3.6	4.5	-	3.6
14	-	4.4	5.0	4.4	4.8	-	4.4

3. 1998 SFRP & GSRP EVALUATION RESPONSES

The summarized results listed below are from the 120 SFRP/GSRP evaluations received.

Associates were asked to rate the following questions on a scale from 1 (below average) to 5 (above average) - by Air Force base results and over-all results of the 1998 evaluations are listed after the questions.

1. The match between the laboratories research and your field:
2. Your working relationship with your LFP:
3. Enhancement of your academic qualifications:
4. Enhancement of your research qualifications:
5. Lab readiness for you: LFP, task, plan:
6. Lab readiness for you: equipment, supplies, facilities:
7. Lab resources:
8. Lab research and administrative support:
9. Adequacy of brochure and associate handbook:
10. RDL communications with you:
11. Overall payment procedures:
12. Overall assessment of the SRP:
13.
 - a. Would you apply again?
 - b. Will you continue this or related research?
14. Was length of your tour satisfactory?
15. Percentage of associates who experienced difficulties in finding housing:
16. Where did you stay during your SRP tour?
 - a. At Home:
 - b. With Friend:
 - c. On Local Economy:
 - d. Base Quarters:
17. Value of orientation visit:
 - a. Essential:
 - b. Convenient:
 - c. Not Worth Cost:
 - d. Not Used:

SFRP and GSRP associate's responses are listed in tabular format on the following page.

Table B-4. 1997 SFRP & GSRP Associate Responses to SRP Evaluation

	Arnold	Brooks	Edward s	Eglin	Griffis	Hanscom	Kelly	Kirtland	Lackland	Robins	Tyndall	WPAFB	averag e
# res	6	48	6	14	31	19	3	32	1	2	10	85	257
1	4.8	4.4	4.6	4.7	4.4	4.9	4.6	4.6	5.0	5.0	4.0	4.7	4.6
2	5.0	4.6	4.1	4.9	4.7	4.7	5.0	4.7	5.0	5.0	4.6	4.8	4.7
3	4.5	4.4	4.0	4.6	4.3	4.2	4.3	4.4	5.0	5.0	4.5	4.3	4.4
4	4.3	4.5	3.8	4.6	4.4	4.4	4.3	4.6	5.0	4.0	4.4	4.5	4.5
5	4.5	4.3	3.3	4.8	4.4	4.5	4.3	4.2	5.0	5.0	3.9	4.4	4.4
6	4.3	4.3	3.7	4.7	4.4	4.5	4.0	3.8	5.0	5.0	3.8	4.2	4.2
7	4.5	4.4	4.2	4.8	4.5	4.3	4.3	4.1	5.0	5.0	4.3	4.3	4.4
8	4.5	4.6	3.0	4.9	4.4	4.3	4.3	4.5	5.0	5.0	4.7	4.5	4.5
9	4.7	4.5	4.7	4.5	4.3	4.5	4.7	4.3	5.0	5.0	4.1	4.5	4.5
10	4.2	4.4	4.7	4.4	4.1	4.1	4.0	4.2	5.0	4.5	3.6	4.4	4.3
11	3.8	4.1	4.5	4.0	3.9	4.1	4.0	4.0	3.0	4.0	3.7	4.0	4.0
12	5.7	4.7	4.3	4.9	4.5	4.9	4.7	4.6	5.0	4.5	4.6	4.5	4.6

Numbers below are percentages

13a	83	90	83	93	87	75	100	81	100	100	100	86	87
13b	100	89	83	100	94	98	100	94	100	100	100	94	93
14	83	96	100	90	87	80	100	92	100	100	70	84	88
15	17	6	0	33	20	76	33	25	0	100	20	8	39
16a	-	26	17	9	38	23	33	4	-	-	-	30	
16b	100	33	-	40	-	8	-	-	-	-	36	2	
16c	-	41	83	40	62	69	67	96	100	100	64	68	
16d	-	-	-	-	-	-	-	-	-	-	-	0	
17a	-	33	100	17	50	14	67	39	-	50	40	31	35
17b	-	21	-	17	10	14	-	24	-	50	20	16	16
17c	-	-	-	-	10	7	-	-	-	-	-	2	3
17d	100	46	-	66	30	69	33	37	100	-	40	51	46

4. 1998 USAF LABORATORY HSAP MENTOR EVALUATION RESPONSES

Not enough evaluations received (5 total) from Mentors to do useful summary.

5. 1998 HSAP EVALUATION RESPONSES

The summarized results listed below are from the 23 HSAP evaluations received.

HSAP apprentices were asked to rate the following questions on a scale from 1 (below average) to 5 (above average)

1. Your influence on selection of topic/type of work.
2. Working relationship with mentor, other lab scientists.
3. Enhancement of your academic qualifications.
4. Technically challenging work.
5. Lab readiness for you: mentor, task, work plan, equipment.
6. Influence on your career.
7. Increased interest in math/science.
8. Lab research & administrative support.
9. Adequacy of RDL's Apprentice Handbook and administrative materials.
10. Responsiveness of RDL communications.
11. Overall payment procedures.
12. Overall assessment of SRP value to you.
13. Would you apply again next year? Yes (92 %)
14. Will you pursue future studies related to this research? Yes (68 %)
15. Was Tour length satisfactory? Yes (82 %)

	Arnold	Brooks	Edwards	Eglin	Griffiss	Hanscom	Kirtland	Tyndall	WPAFB	Totals
# resp	5	19	7	15	13	2	7	5	40	113
1	2.8	3.3	3.4	3.5	3.4	4.0	3.2	3.6	3.6	3.4
2	4.4	4.6	4.5	4.8	4.6	4.0	4.4	4.0	4.6	4.6
3	4.0	4.2	4.1	4.3	4.5	5.0	4.3	4.6	4.4	4.4
4	3.6	3.9	4.0	4.5	4.2	5.0	4.6	3.8	4.3	4.2
5	4.4	4.1	3.7	4.5	4.1	3.0	3.9	3.6	3.9	4.0
6	3.2	3.6	3.6	4.1	3.8	5.0	3.3	3.8	3.6	3.7
7	2.8	4.1	4.0	3.9	3.9	5.0	3.6	4.0	4.0	3.9
8	3.8	4.1	4.0	4.3	4.0	4.0	4.3	3.8	4.3	4.2
9	4.4	3.6	4.1	4.1	3.5	4.0	3.9	4.0	3.7	3.8
10	4.0	3.8	4.1	3.7	4.1	4.0	3.9	2.4	3.8	3.8
11	4.2	4.2	3.7	3.9	3.8	3.0	3.7	2.6	3.7	3.8
12	4.0	4.5	4.9	4.6	4.6	5.0	4.6	4.2	4.3	4.5
Numbers below are percentages										
13	60%	95%	100%	100%	85%	100%	100%	100%	90%	92%
14	20%	80%	71%	80%	54%	100%	71%	80%	65%	68%
15	100%	70%	71%	100%	100%	50%	86%	60%	80%	82%

A SIMULATION STUDY OF THE VULNERABILITIES
IN COMMERCIAL SATELLITE CONSTELLATIONS

Sang Ho Bae
Graduate Student
Department of Computer Science

University of California, Los Angeles
Los Angeles, CA

Final Report for:
Graduate Student Research Program
Rome Research Site

Sponsored by:
Air Force Office of Scientific Research
Bolling Air Force Base, DC

And

Rome Research Site

September 1998

A SIMULATION STUDY OF THE VULNERABILITIES
IN COMMERCIAL SATELLITE CONSTELLATIONS

Sang Ho Bae
Graduate Student
Department of Computer Science
University of California, Los Angeles

Abstract

A simulation study of vulnerability in commercial low earth orbit satellite constellation has been conducted. Increasing number of satellite constellations are being set in place in the earth orbit by various companies. Availability of these resources has prompted the study of possible military application during the emergency situation. The simulation is designed to measure the performance drop of Globalstar constellation in a hostile environment. In the presence of jamming transmission, up to 56 percent of transmission per satellite was lost. A method to detect hostile transmission and allow the transmission to hand off from effected satellite to other satellites in the constellation has to be developed if such constellations are to be used in military application.

A SIMULATION STUDY OF THE VULNERABILITIES IN COMMERCIAL SATELLITE CONSTELLATIONS

Sang Ho Bae

Introduction

In the past decade, a number of companies have ventured to develop personal satellite communication based on Low Earth Orbit (LEO) satellite technology. These plans are today maturing into satellite constellations that span the globe. One of the companies, Iridium, has already placed all the satellites in orbit and is ready to activate the test run in a near future. It is not very surprising to see such rapid pace in the development stage of these ventures since the companies are relying on proven technology to develop and launch the system. Geosynchronous Earth Orbit (GEO) satellites have two noted disadvantages if they are to be used for personal communication. These stem from the distance between the user and the satellite that is required to keep the satellite geographically static. First, it requires a strong transmission, which demands high power consumption. Second, the end to end propagation delay makes the personal communication in real time somewhat difficult [6]. On the other hand, LEO satellites require lower power and provide smaller delay. LEO satellites solve the problems unique to GEO satellites, but LEO satellites are not synchronous to the geographic location. In order to perform the task equivalent to single GEO, there has to be multiple LEO satellites following the same orbit with appropriate signal handoff protocols so the transmission may continue even though satellite which established the connection originally have moved out of the area. When enough number of these LEO satellites is in place with calculated phase shift, global coverage can be achieved [3,5]. In emergency situations, such systems can serve to replace or compliment the satellite systems currently used by the military, but they lack the security precautions taken by the military counterparts and are quite vulnerable in hostile environment. In this paper, a scenario of such hostility against the satellite following the orbital information of Globalstar satellite constellation is analyzed through the simulation.

Methodology

Satellite Took Kit (STK) satellite simulation test bed has been used to generate the simulation scenario and to generate the transmission data from the user to the satellite constellation. The generated data is post-processed with Microsoft Excel to yield comparative result.

1. Scenario

STK requires minimum of three basic objects within the scenario. First it requires a map of the given world where scenario will run. Second, it requires a satellite, which orbits around the world, and lastly, it requires a target which satellite is transmitting and/or receiving signal with [1]. For the simulation, a map of earth is used, but only a limited coverage area has been defined since simulating over the entire map area

will be quite complex. Within the coverage area, a facility is placed equipped with a transmitter that has a wide frequency bandwidth and the high enough power to interfere with any possible transmission from ground to the satellite. The satellite follows the orbital information given by the Globalstar system. The Globalstar system has 48 low earth orbit satellites in eight planes where the planes divides the earth sphere equally [7]. Each satellite has a 1414-kilometer circular orbit inclined at 52 degrees. The satellite is three-axis stabilized and consists of a trapezoidal main body, two deployable solar arrays and a deployable magnetometer on a boom. Unlike many geosynchronous satellites, the antennas are not deployable. The heart of a Globalstar satellite, its communications systems, consists of two sets of antennas. C-band antennas are for communications with Gateways, and they operate with 5091-5250 MHz bandwidth for gateway-to-satellite communication and 6875-7055 MHz bandwidth for satellite-to-gateway communication. L- and S-band antennas are used for communication with user terminals, and they operate at 1610-1626.6 MHz bandwidth for user-to-satellite transmission and 2483.5-2500 MHz bandwidth for satellite-to-user transmission [3]. The constellation is designed for 100% single satellite coverage between ± 70 latitude, and 100% dual or higher satellite coverage between 25 to 50 latitudes. Globalstar will employ path diversity combining to mitigate blocking and shadowing; up to three satellites may at any one time be used to complete the call [7]. In the simulation, it has been assumed that the jammer effects only the L-band antennas used in user-to-satellite transmission, which has fixed array with fixed array with 16 beams, depicted in figure 1. To actually denote the performance drop due to the transmission interference from the

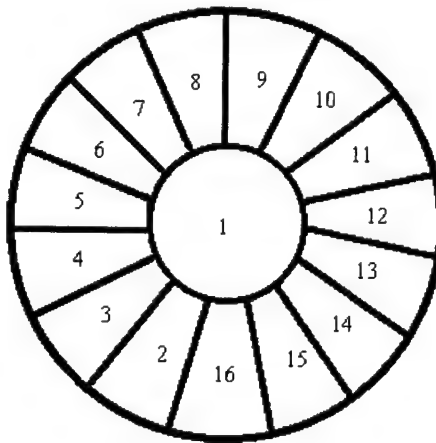


Figure 1. L-band satellite antenna configuration footprint: typical 16 beams fixed array

jammer station, two identical satellite is placed in the orbit occupying the same time and space. One of the satellites depicts the normal operation of the satellite where satellite tracks the user signal without any ground bound interference from the jamming facility. The other satellite tracks only the interference signal

of the jamming facility disregarding the user signal. The tracking of the signal is simulated in the simplest manner by having the access enabled whenever transmitter covered by the sensor array pattern of the satellite. Both the user and the jammer facility are located within the coverage area. The coverage area is placed around an island off the coast of Brazil at Atlantic Ocean. The jammer facility is placed on the island itself, and the primary target for the satellites is the transmitter located on the ship near the island. The area has been designed to simulate the situation where hostilities by the rebel forces have overturned the control of the island and a warship has been sent by the military to deal with it. Since the entire communication link from the island to the mainland has been fallen under the rebel control, friendly forces at the ocean must rely on the satellite communication. The GEO satellite has been somehow disabled and to establish a direct communication link with the command center located back in US, LEO satellites orbiting within the area are being used. Eight satellites are placed in the simulation. Four satellites depict the actual satellites within the Globalstar constellation. The other four satellites are their counterparts with duplicated orbiting constants tracking the jamming facility. The orbital constants of these models are based on the orbital constants of the Globalstar satellites that are currently in orbit. Each satellite has an antenna configuration pattern depicted above. The time period of the simulation is chosen so that the satellites will converge and their antenna pattern will overlap at the coverage area. With multiple satellites in the area, it is possible for the user transmission to be picked up by at least one of the receivers even with the presence of the jammer. Using the STK's access report generator, data of time intervals where each sensor of the satellites has the access to either the user transmitter or the interference generator in the jammer facility has been recorded.

2. Post-processing

It is hard to give meaning to the raw data gathered by STK reports. The data gathered from the above scenario is reprocessed and reorganized using the Microsoft Excel in this stage. All the user transmission access intervals for each satellite are gathered into single Excel sheet and the corresponding jammer transmission to the counter part satellites are also entered in matching raw. The intersecting jammed intervals are deducted from the user transmission interval leaving only the interval where no interference exists. The amount of interval with jamming transmission is compared with jam-free transmission and efficiency is calculated. Figure 2 depicts a reduced sample of a typical STK access report for satellite tracking the jammer transmission. First and second columns of the report list the sensor identifier and the transmitter source listed sensor is tracking. Second and third columns list the duration of access interval.

```
12 Aug 1998 13:29:27
Facility-Jammer-To-Satellite-tle-2516375jm-Sensor-Sensor7510j, Sensor-Sensor7511j,
Sensor-Sensor7512j, Sensor-Sensor7513j, Sensor-Sensor7514j, Sensor-Sensor7515j, Sensor-
Sensor7516j, Sensor-Sensor7517j, Sensor-Sensor752j, Sensor-Sensor753j, Sensor-Sensor754j,
Sensor-Sensor755j, Sensor-Sensor756j, Sensor-Sensor757j, Sensor-Sensor758j, Sensor-
Sensor759j
```

No Access Found

7511j - To Object	7511j - From Object	7511j - Start Time	7511j - Stop Time
-----	-----	-----	-----
To Sensor 7511j	From Jammer	1 Jan 03:01:54.20	1 Jan 03:03:36.45

7512j - To Object	7512j - From Object	7512j - Start Time	7512j - Stop Time
To Sensor 7512j	From Jammer	1 Jan 00:57:46.25	1 Jan 01:02:04.66
To Sensor 7512j	From Jammer	1 Jan 02:58:20.25	1 Jan 03:03:04.20
7513j - To Object	7513j - From Object	7513j - Start Time	7513j - Stop Time
To Sensor 7513j	From Jammer	1 Jan 00:55:27.84	1 Jan 00:58:48.57
To Sensor 7513j	From Jammer	1 Jan 02:56:52.78	1 Jan 02:59:01.30
7514j - To Object	7514j - From Object	7514j - Start Time	7514j - Stop Time
To Sensor 7514j	From Jammer	1 Jan 00:53:40.03	1 Jan 00:56:10.50
To Sensor 7514j	From Jammer	1 Jan 02:55:40.37	1 Jan 02:57:01.60
7515j - To Object	7515j - From Object	7515j - Start Time	7515j - Stop Time
To Sensor 7515j	From Jammer	1 Jan 00:51:31.00	1 Jan 00:54:16.50
To Sensor 7515j	From Jammer	1 Jan 02:54:10.75	1 Jan 02:55:45.50
7516j - To Object	7516j - From Object	7516j - Start Time	7516j - Stop Time
To Sensor 7516j	From Jammer	1 Jan 00:48:11.81	1 Jan 00:52:24.03
To Sensor 7516j	From Jammer	1 Jan 02:51:16.95	1 Jan 02:54:29.75
7517j - To Object	7517j - From Object	7517j - Start Time	7517j - Stop Time
To Sensor 7517j	From Jammer	1 Jan 00:47:25.82	1 Jan 00:47:25.90
To Sensor 7517j	From Jammer	1 Jan 02:48:53.00	1 Jan 02:52:35.20
No Access Found			

Figure 2. Access report for transmission access between satellite 75 and Jammer Facility

In the table 1, a reduced sample of the spreadsheet used to calculate the result has been presented. On

Sensor ID	Start time	Stop time	Jam start	Jam stop	User accs start	User accs stop	Duration
13	00:00:00	00:00:00	02:58:14	02:59:01	00:00:00	00:00:00	00:00:00
14	00:00:00	00:00:00	02:55:40	02:57:02	00:00:00	00:00:00	00:00:00
15	00:00:00	00:00:00	02:54:11	02:55:46	00:00:00	00:00:00	00:00:00
17	00:47:25	00:51:34	00:47:26	00:47:26	00:47:25	00:51:34	00:00:00
16	00:50:14	00:53:51	00:48:12	00:52:24	00:47:25	00:53:51	00:00:00
15	00:53:20	00:55:16	00:51:31	00:54:17	00:47:25	00:55:16	00:00:00
14	00:55:02	00:56:43	00:53:40	00:56:11	00:47:25	00:56:43	00:00:00
13	00:56:24	00:58:03	00:55:28	00:58:49	00:47:25	00:58:59	00:00:00
12	00:58:03	01:02:52	00:00:00	00:00:00	00:47:25	01:02:52	00:15:27
17	02:48:53	02:54:25	02:48:53	02:52:35	02:48:53	02:54:25	00:05:32
16	02:54:25	02:55:04	02:51:17	02:54:30	02:54:25	02:55:04	00:00:00
2	02:54:26	02:58:43	00:00:00	00:00:00	02:54:25	02:58:43	00:00:00
12	02:58:14	03:01:54	02:48:14	03:01:07	02:54:25	03:01:54	00:00:00

11	02:59:41	03:05:22	03:01:54	03:03:36	02:54:25	03:05:22	00:10:57
Total access duration with jamming 00:22:12			Total access duration 00:31:16				
<u>Total access duration with jamming</u>			X 100% = Percent Total 70.99 %				
Total access duration			Of the original interval				

Table 1. Sample spreadsheet calculation for transmission access between satellite 75 and Jammer Facility

first column the sensor identifier number is listed. Second and third columns list the time interval where sensor accesses the user transmission. Columns four and five indicate the time interval where user transmission has been jammed by interference. Columns six and seven denote the total accumulated intervals of time where user transmission is accessed when there is no interference signal. The intervals are accumulated at the last column. Same method is used to accumulate the intervals where interference is present, but the columns are omitted due to the space limitation.

Results

The results for the individual satellite access performance calculations and the result for the multiple access of the user by all four satellites are listed in the Table 2. On average, the satellites retained only forty-seven

Satellite ID	Total access duration with jamming (minutes:seconds)	Total access duration without jamming (hours:minutes:seconds)	Percent Total (%)
3	00:00	00:04:57	0.00
65	11:46	00:27:21	43.03
75	22:12	00:31:16	70.99
86	23:22	00:30:21	77.02
Multiple access	39.36	01:04:56	60.98

Table 2. Satellite access performance comparison with and without the jammer interference

percent of the user transmission access interval prior to jammer interference, but it is worthy to note that nearly half of the original transmission interval has remained accessible. Also, the percentage above only indicates the average comparison of the user transmission access of individual satellites based on the access time reduction caused by the jammer interference. While individual access interval has been reduced to forty-seven percent, total access of four satellites has only been reduced to sixty-one percent. That is, from the original user transmission access interval of all the satellites, for sixty-one percent of the time, at least one of the satellites were unaffected by the jammer interference.

Future Works

The scenario is to be further improved by using the Programmer's Library (PL) module of the STK. With the current sensor tracking system, the moment sensor come in contact with the jammer transmitter, the user transmitter signal is lost completely. This, of course, is not realistic. There has to be a cross over of the signal dominance where the user's signal becomes unrecognizable due to the increase in signal strength

of the hostile transmission as the satellite move toward the jammer facility. Using PL module, this boundary limitation algorithm can be incorporated into the calculation stage of the access report. The post-processing also needs to be improved by automating the steps currently is being done manually. The post-processing steps can all together be eliminated by moving and incorporating the calculations carried out with Excel into the STK access report processes themselves using the PL module. Ultimately, the report generated by STK should be able to stand on it's own and provide the user a meaningful data.

Conclusion

LEO satellite constellation provides a convenient medium for communication. In the areas without prior development, laying out a communication infrastructure from a scratch is not cost effective and for the area where the such system does exist, LEO satellite constellations provides a convenient backup in emergency situations. Same idea applies in the military applications. Military personnel often find themselves in locations where regular communication medium is not accessible. GEO satellites can be used for transmissions where latency caused by propagation does not matter, but for most end-to-end digital communications, minimum round-trip latency of 500-millisecond [6] is not acceptable. LEO constellation provides a good alternative with a negligible delay. To be used in military application, Globalstar LEO constellation has been simulated on the STK testbed to test the performance. In the simulation, the constellation retained up to sixty-one percent of the original access interval with the presence of the interference transmitter in the immediate area since the constellation has multiple coverage of the area. The performance is promising, but it has to be noted that only with multiple coverage of the constellation as the whole has allowed the system to retain much of the access interval where as some of the individual satellite has dropped down to zero percent. In order for user transmission to be received accurately, one of two following protocols has to be applied. First, the satellite has to be able to detect the clarity of the user signal and have ability to hand off to another satellite when the clarity of the signal drops below the threshold. This will allow the transmission to continue even if some of the satellites are disabled due to interference. Another, more simpler, approach will be to have all the satellites that can receive the signal clearly receive it simultaneously and forward them to ground station where the signals will be processed. The signals can be processed simply either by taking the consensus or by measuring the signal strength and selecting the best one. Ground station possesses higher computational power so this can be carried out without expanding the satellite capability. The results of the current simulation are far from being accurate due to signal measurement algorithm currently being used. Much work is needed to precisely simulate the signal strength and interference signal.

References

1. Analytical Graphics, STK User's Manual, Analytical Graphics Incorporated, 1997
2. G. Garriott, "Low Earth Orbiting Satellites and Internet-Based Messaging Services", Proceedings of ISOC conferences 96, via World Wide Web,
http://info.isoc.org/isoc/whatis/conferences/inet/96/proceedings/g1/g1_1.htm , 1996
3. Globalstar Technology, "Globalstar Technology", via World Wide Web,
<http://www.globalstar.com/tech/tech.htm>, Aug 1998
4. R. Jenoso, Performance Analysis of Dynamic Routing Protocols in a Low Earth Orbit Satellite Data Network, Master's Thesis, Air Force Institute of Technology, 1997
5. Teledesic Technology, "Technical Overview of the Teledesic Network", via World Wide Web,
<http://www.teledesic.com/tech/details.html>, Aug 1998
6. Teledesic Technology, "Does Latency Matter" , White Paper via World Wide Web,
<http://www.teledesic.com/tech/latency.html>, Sep 1998
7. L.Wood, "Big LEO overview", via World Wide Web,
<http://www.ee.surrey.ac.uk/Personal/L.Wood/constellations/tables/overview.html>, Aug 1998

**NEAR-OPTIMAL ROUTING OF
UNMANNED SURVEILLANCE PLATFORMS**

Keith R. Buck

Department of Mathematics

Colorado State University

Fort Collins, CO 80523

Final Report for

Graduate Student Research Program

Rome Research Site

Sponsored by

Air Force Office of Scientific Research

Bolling Air Force Base, DC

and

Rome Research Site

August 1998

**NEAR-OPTIMAL ROUTING OF
UNMANNED SURVEILLANCE PLATFORMS**

Keith R. Buck

Department of Mathematics

Colorado State University

ABSTRACT

Many issues still need to be explored in the field of sensor management. Real battle scenarios introduce many physical complexities for consideration. In this paper, we begin to explore sensor resource scheduling by looking at the problems involved in routing of surveillance platforms. Unlike many classical routing problems, surveillance platforms must view each target or region of interest rather than visiting it. Terrain obscuration and other similar constraints add many new complexities to this problem. We therefore propose a visibility-constrained routing problem. In general, the solution may be quite different from the problems posed by previous works. The value of the sensor platform may be increased greatly by using a routing scheme which takes visibility into account.

For this study, we use a specific example from the Off-board Augmented Theater Surveillance (OBATS) project at Rome Research Site. An unmanned air vehicle (UAV) may be used for surveillance or target identification purposes. The UAV simulation used in the OBATS lab has been modified to allow for implementation of solutions to an example routing problem. A mathematical model for routing of an independent, self-tasking UAV has been formulated. Final work will include the application of Lagrangian relaxation-based methods to this NP-hard problem. Refinements to the physical model will include multiple UAV's, realistic flight dynamics, threat avoidance, and time constraints.

**NEAR-OPTIMAL ROUTING OF
UNMANNED SURVEILLANCE PLATFORMS**

Keith R. Buck

1 Introduction

This report is a result of my work in the 1998 AFOSR summer research program. It describes interim results of an ongoing research effort at Colorado State University in cooperation with Rome Research Site. The purpose of this research effort is to explore the use of multi-dimensional assignment techniques and Lagrangian relaxation in the areas of sensor resource management, scheduling, and allocation as it relates to the Off-Board Augmented Theater Surveillance project (OBATS). As a first step in this direction, we look at optimal routing of unmanned air vehicles (UAV's), which may be used to observe or identify targets. In particular, some routing problems must take into account terrain obscuration, and this leads us to visibility constraints, which introduces significant variations on traditional routing problems.

The UAV's may wish to identify or scan different targets to contribute to overall battlespace awareness. Using an accurate model for visibility may allow for the computation of much more efficient flight paths, but this area seems to be relatively unexplored. Most work relating to optimal flight paths thus far has focused on flying between two points, rather than looking at the overall mission. We plan to explore the use of Lagrangian relaxation based algorithms to find near-optimal solutions to this extremely complex problem.

A formal mathematical model for this preliminary problem has been developed, and is described in section 4.2. UAV simulation software from the OBATS lab has been modified to allow for algorithm testing. We are implementing and will test both a greedy algorithm and a Lagrangian relaxation-based algorithm in this software. Next, we will modify the basic problem to include many of the physical complexities inherent in any real battle scenario. At each step, we will re-solve the problem to test the effectiveness of our techniques.

OBATS is being developed to allow for the exchange of information between multiple surveillance platforms [2]. Enhanced multi-platform surveillance and information fusion will increase the possibility for accurate mobile target engagement. Currently, the proposed architecture is completely distributed, so no platform can have control of or directly task any

off-board resources. Each platform has its own mission to accomplish, and is unable to dynamically service requests which would require a change in flight plan.

By adding an independent UAV whose sole purpose is to dynamically service requests for other platforms, operators can obtain more of the information they need. UAV's do not have on-board operators requesting information, so they are able to freely satisfy off-board requests. We would like to automatically route these surveillance platforms to maximize their effectiveness. As our first approximation to this problem, we attempt to minimize the total distance which the UAV travels while viewing each requested region. This yeilds a significantly different and unexplored variant of traditional routing problems, where the platform needs to view each destination from a safe distance rather than travel to it. Future enhancements to the problem will include multiple UAV's, time constraints, realistic flight dynamics, and priorities. (For a discussion of some of these issues, see [3] or [1].)

The organization of this paper follows a fairly standard format. Section 2 gives some technical background, and describes the basic motivation for this research. It then describes a specific example which will be used for illustration purposes and discusses some theoretical aspects of the problem. Section 3 describes UAV simulation software and its eventual use to test solutions to the problem. Section 4 describes our current status, some future work, and the mathematical model which has been developed.

2 Discussion of Problem

2.1 Background

The AWACS platform is designed to provide surveillance of a given airspace. It has a radar sensor which scans every direction on a rotating basis. The aircraft flies in a fixed circuit outside the battle zone. This platform provides air situational awareness.

Just as AWACS watches over the battle in the air, the Joint STARS aircraft oversees the battle on the ground. Joint STARS supports an entire campaign through surveillance and information management. During the mission, the aircraft follows a pre-planned flight path. At certain intervals, it must turn around to stay within range of the battle. During turns, the radar actually flips over to view the other side of the aircraft, enabling surveillance while the aircraft flies in both directions. A blind spot exists, however, while the radar switches sides. There are also blind spots due to terrain visibility restrictions, especially because the aircraft must stay away from the battle to avoid being shot down. Other resources must be used to fill in this data.

The Rivet Joint aircraft serves a third purpose. All types of electronic data, including SIGINT, COMINT, and ELINT, are managed by operators on board. SIGINT is the monitoring of enemy signals, including radio waves and other types of transmissions. COMINT involves the listening in on enemy communications to anticipate future tactics. ELINT data enables the operator to locate certain electronic devices such as weather radar stations and other active surveillance devices.

In the future, much of the work of these surveillance platforms will be done by Unmanned Air Vehicles (UAV's). The advantages of a UAV include higher and longer flight availability, extra maneuverability, and extra availability without risk of loss of life. The purpose of the UAV is to provide additional surveillance capabilities without the constraints imposed by a manned vehicle.

For this effort, we will assume that a UAV could house a Moving Target Indicator (MTI) radar sensor, similar to the current Joint STARS sensor. The MTI sensor uses a Doppler radar to detect objects which are moving faster than a given velocity threshold. It can distinguish certain types of targets and measure the sizes of objects. Once an area has been scanned, certain classes of targets can then be designated as a high priority. Another UAV may then

fly to a close range to identify or better locate the target.

Representative classes of targets which may need identifying include radar emitters, mobile missile launchers (transporter erector launchers, or TEL's), and rotating antennas. A proposed con-ops for a missile launch begins with the activation of a mobile radar station to pinpoint location and check the weather. An ELINT detector will give an approximate location for the radar emission, but ELINT data is not very accurate. Static movers are objects which return a Doppler signature to a MTI radar, but do not change position. This is generally associated with a rotating radar antenna, and the correlation with ELINT data gives a good indication of position. There is a sequence of operations which must occur before launch, and this process takes about half an hour. Before that happens, we would like to identify and destroy the launcher.

2.2 Motivation

The Off-Board Augmented Theater Surveillance (OBATS) project is being designed to allow for the fusion of information from multiple platforms [2]. The basic architecture allows for multiple nodes, each of which may request certain off-board information, and may receive and service requests from other OBATS nodes. OBATS nodes are completely distributed; no hierarchy of nodes exists. No node can require that another node service a given request.

This type of distribution is desired in any system used in a real-life battle scenario to avoid single points of failure. The purpose of OBATS is to provide information to operators connected to one node from sensor resources connected to other nodes. To get this information, the user must request it from his or her console. This request is then sent to the platform most likely to be able to service it. The other platform may or may not be able to service the request, and the option is always left open to deny a request for any reason. No operator is able to command another platform to perform some operation. An extreme example of an off-board operator's inability to have control is when the other platform has been shot down or has crashed.

A totally distributed system such as OBATS can only work when off-board platforms willingly service as many requests as possible. Most platforms already have a mission and must fulfill their own requests first. To solve this problem, we can introduce a UAV whose primary purpose is to supply existing platforms with extra information by satisfying off-board

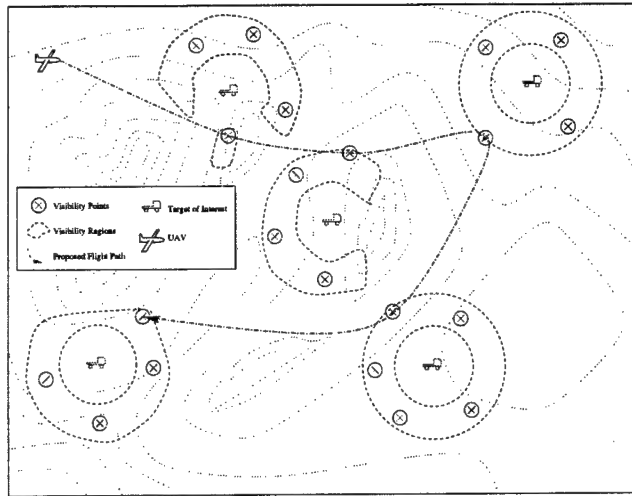


Figure 2.1: Terrain restrictions and the visibility-based TSP

requests. We would like to task this UAV as efficiently as possible so as to maximize its effectiveness. There are several problems which need to be explored which relate to tasking this UAV, including routing, scheduling, and sensor management. Each of these problems has far-reaching applications to other routing and scheduling problems which are beyond the scope of this paper.

2.3 Routing

The routing problem as it applies to a UAV is the process of determining where the aircraft should go. For our purposes, we will assume that a list of regions to scan is given. The UAV must then scan each region while traveling a minimal distance. At first glance, this sounds like a Traveling Salesman Problem (TSP), one of the most famous routing problems in existence. This problem, however, displays characteristics which make it very different from the classical TSP.

In the traditional TSP, the salesman is required to visit each one of the cities, which are represented by vertices on a weighted graph. In most situations involving surveillance, the sensor is not required to actually “visit” each location. Instead, the sensor just needs to be able to scan the target. In fact, it may be desirable to stay a safe distance away from the target. This leaves open the possibility that the “cities” in the traditional problem are now spatial entities with non-zero dimensions. The ability to view a target from an entire region

may decrease the minimum travel distance considerably. It may also alter the order in which targets should be visited (see section 2.7).

There are several other complexities in this physical problem which differentiate it from the classical TSP. In the battlefield scenario, certain points need to be avoided, such as those near surface-to-air missiles (SAMs). Avoidance points can be added within the context of the TSP by modifying the distance function to include non-linear flight paths. In some cases, detours to avoid danger areas may also change the optimal route order, because the UAV will be closer to some targets just because it is attempting to avoid another area.

There may also be direction of travel restrictions based on the terrain or foliage present to maximize the probabilities of detection. Limited fuel capacity may induce a desire to minimize the number of maneuvers, and the flight dynamics of the specific aircraft will influence a minimal energy flight path. Restrictions such as direction of travel and aircraft characteristics require substantial modifications to the classical problem. The cost of traveling from one location to the next becomes a function of the last location visited and the next, causing an additional combinatorial explosion of possibilities.

Another complexity which may be added to this problem is that of critical targets (also called “must-do” tasks). While some targets should be visited just to add to overall battlefield awareness, other targets are critical to a successful campaign. For example, it is nice to know where every enemy vehicle is located, but it is more important to identify one TEL about to destroy a city than to monitor hundreds of enemy trucks, and the UAV should be tasked accordingly. A flight path should be calculated which maximizes the number of critical targets and then modified to include as many less important targets as possible without changing the number of critical targets visited. This, then, starts out as a basic routing problem in the style of the TSP, but has additional soft goals to consider as well.

2.4 Platform Scheduling

There are other real-world needs which make this problem different from the traditional TSP. In an actual battlefield scenario, time is an important factor. This may affect the UAV in several different ways. For example, some targets may need to be scanned sooner than a certain time. This may occur when a missile is about to be launched; the artillery needs to destroy the launcher before that happens, but the target must be identified by the UAV before

it can be targeted. The consideration of time constraints increases the difficulty of the basic routing problem by adding a scheduling aspect.

There are several considerations in a scheduling problem. Usually, a scheduling problem is denoted by a list of jobs and precedence constraints. In surveillance theory, however, the only precedence constraints are generally of the form that we must know a target exists before scheduling it to be identified. Thus, the usual precedence constraints have already been satisfied before we begin to optimize a schedule. We do not attempt to add a target to our schedule until we already know that it exists.

In many surveillance problems, a time window for each request may be specified instead. This means that each request would have an associated start and end time, with the requirement that the task be serviced within those times. The goal is then to schedule requests to be satisfied in some optimal way. There are several possibilities:

1. Minimize the number of unsatisfied requests.
2. Minimize the overall distance between the service time and the requested time window.
(i.e. there may be some value to satisfying requests even if they missed their time window slightly)
3. For a one-sided window, minimize the time between the request time and the service time.
4. Requests may be given relative priorities which allow several semi- important tasks to outweigh one higher priority task. There are many possibilities of objective functions which use some formula to determine which sets of requests should be serviced to maximize the benefit of the platform.

2.5 Sensor Scheduling

Another issue related to automatically tasking UAV's is scheduling the individual sensor. It is necessary to make decisions relating to the sensor independently of the platform because a given platform may have more than one sensor on-board. Thus, given a list of requests to service and a platform position (as a function of time), a sensor scheduler must determine which

direction the sensor should point next. There are many factors to be considered, including but not limited to:

- Type of sensor (Radar, IR, electro-optical, etc.).
- Physical characteristics of casing around the sensor.
- How scanning is controlled (physical gimbal or electronically steered).
- Sensor mode.
- Time required to change mode.
- Time required to move the sensor.
- How many regions can be simultaneously scanned in a given sensor mode.

Each of these factors affects a proper sensor schedule significantly. To choose a proper scheduling algorithm, only the designer of the sensor will have enough information. The general classes of algorithms used to schedule sensors are the same as those algorithms which schedule disk I/O on computers. They include techniques such as first-come, first-serve and shortest job time first. For a further description of these principles, see [4]. Throughout the rest of this paper, we will assume that the sensor manufacturer has chosen the correct sensor scheduler. The sensor is therefore capable of servicing all of the important requests in visible range of the aircraft.

2.6 A Specific Example

For the purposes of initially demonstrating some methods of solving these types of problems, we now choose a specific example problem to solve. Further research will need to include more complexities which are inherent in the real scenario. Implementation will need to focus on issues such as specific parameter values. For now, we confine ourselves to the simplest example possible which still generates an interesting problem.

Suppose we are given a set of locations on the ground where we are told that certain types of targets may exist. Given an elevation map of the terrain, we can compute several aerial positions from which we may view each ground location. A region of visibility for each ground

location may be continuous. For the purposes of this problem we will discretize the space in such a way as to find a few key positions from which the platform will have a good view of the area. We will call this a set of visibility points. These points may be chosen in such a way so as to add robustness to the solution by eliminating those points from which the platform could no longer see the target if it moved slightly. This also limits the possible tours to a finite (though extremely large) number.

We will assume for now that the UAV flies at a constant altitude and has a constant speed so that travel time is directly proportional to Euclidean distance in two dimensions. We will also assume that the UAV can change direction instantaneously, so that the solution is independent of any specific flight dynamics. Our task then, is to determine a minimal distance route which will ensure that we can view each ground location. This means that the UAV must visit at least one aerial position in each set of visibility points. We will call this the “visibility-based TSP.”

2.7 Theoretical Aspects

A restatement of the classical TSP is to find a minimum Hamiltonian circuit on a complete, weighted graph. The vertices correspond to cities and the weights of the edges correspond to the cost of travel between the two cities (this may be in distance or dollars). A Hamiltonian circuit is a tour which visits all of the vertices exactly once and then returns to the starting point. The goal is then to minimize the total weight of the edges used in this circuit.

For the visibility-based TSP, we also wish to find a minimum circuit on a complete, weighted graph. The graph is defined similarly, with the vertices corresponding to visibility points, and the weights of the edges correspond to the distance between the points. The main difference is that the circuit is only required to visit one visibility point for each ground location. The circuit is a solution to the TSP on a subgraph containing exactly one visibility point from each set.

If there were only one visibility point for each ground location, then the visibility-based TSP reduces to the classical TSP. Thus, the visibility-based TSP is a generalization of the classical TSP, and is therefore also NP-hard. In general, the optimal solution will be different, and the optimal route will have a different order than the optimal route for the classical TSP. For example, in figure 2.2, the middle target should be visited between the top two targets

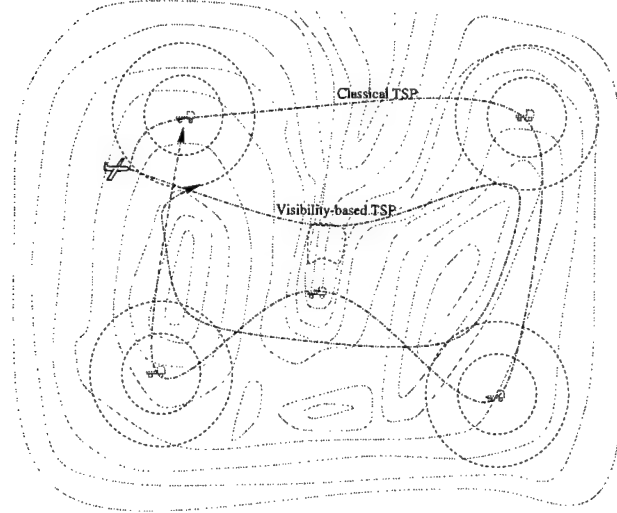


Figure 2.2: Comparison of TSP vs. Visibility-based TSP

based on visibility, but would be visited between the bottom two targets in a classical TSP.

It is worthwhile to note that there exists a continuum of difficulty levels. If the UAV flies at a very high altitude, has a long-range sensor, and the terrain is very flat, then routing of the UAV is trivial. The sensor can see the targets no matter where the platform is located. It is much more important to point the sensor in the right direction than to worry about flight dynamics. If, on the other hand, the sensor has an extremely short range or the UAV is flying at an extremely low altitude, then the optimal flight path is approximately the same as the optimal path for the classic TSP.

In the middle of these two extremes, the problem is much more complex. If the UAV flies low enough that terrain is an issue, but high enough to still view targets at a reasonable distance, then taking visibility regions into account can change the flight path dramatically. Also, in some proposed scenarios, a UAV might fly in stealth mode (at a very low altitude to avoid detection) for most of its mission, then pop-up to take a look at a region of interest. To avoid any extreme changes in altitude, the plane should still get to one of a few good vantage points, pop-up to take a look at the region before returning to stealth mode. Thus, depending on the specific combat scenario, this problem may be either trivial or very complex.

3 Methodology

As part of the OBATS project, a UAV simulation has been developed. The software includes realistic combat scenario input and a set of simulated UAV's. The UAV's have a virtual MTI Radar on-board, with specifications given by a parameter file. The simulation uses actual terrain data to determine whether or not a target is visible to the UAV. In some mountainous regions, there are very few visibility points for each target.

Originally, the UAV's could be tasked by giving a destination and a way-point. The UAV would fly close to the way-point en route to its destination. After reaching the destination, the UAV would continue in a straight flight path until re-tasked. The simulation now includes the capability to task a UAV to fly around continually in a fixed orbit, scanning one direction at all times. This is similar to a Joint STARS flight path, which can provide for overall situational awareness. These task types provide the basic infrastructure for the generation of several different types of problems.

The ability of a UAV to automatically task itself is critical to the testing of solutions to the visibility-based TSP. For the purposes of this study, a module has been added which uses the targets in the simulation to task the UAV. There are hundreds of targets in the simulation. Several key targets, such as TELS, are chosen to be identified. Visibility points can then be calculated based on the terrain, and the algorithm to be tested can choose the path of the UAV.

In real implementations, the actual location of the targets will not be known. Visibility points must be chosen which allow for a margin of error in the target's position. Alternatively, input may be a request to scan a certain region, and visibility points would be chosen which ensure a certain percentage of the region can be seen. Each of these real-life scenarios fit within the context of the basic problem. Certain visibility points need to be visited by the UAV in a minimal amount of time. The test environment provides an easy way to supply somewhat realistic points which need to be visited.

Most real-time scheduling systems use some sort of heuristic greedy method. This means that whichever option looks best at the current time will be chosen, without respect to future possibilities. This type of algorithm is generally fast and can come up with a solution in polynomial time. Sometimes, the solution is even somewhat close to optimal. Usually, however,

a global optimization approach will do much better.

For comparison purposes, the first solution to this problem we will use will be a greedy method. Starting at an arbitrary visibility point, we find the next closest point which will allow the UAV to see a different target. After eliminating these targets from our list, we then find the closest visibility point corresponding a remaining target. We repeat this procedure until all targets have been eliminated. The UAV then returns to its starting point. This method quickly produces a tour touching one visibility point per target.

Next, we plan to use a Lagrangian relaxation-based method to find a better solution. Basically, this involves formulating the problem as the minimization of some objective function subject to some inequality constraints. We then relax one or more constraints and solve the relaxed problem using Lagrange multipliers. As a final step, we try to modify the resulting solution to fit the original constraint set without significantly changing the optimal value. If we succeed, then we have a near-optimal solution to the original problem. Otherwise, we must relax a different set of constraints. This method has worked well in the past on several problems, including the classical TSP.

4 Results

4.1 Current Status and Future Plans

This work is part of ongoing research. Although much has been accomplished thus far, there are also many areas which will need to be explored. To date, our effort has been focused on finding a well-defined, well-posed problem which can be applied to sensor resource management. A mathematical model has now been formulated (See section 4.2). We have also modified simulation software to allow for the testing of potential solutions to the problem.

As discussed in previous sections, the problem we have formulated so far is of minimal complexity, but still addresses several theoretical issues. We assume ideal sensors and flight dynamics as well as preprocessing of the problem to form an associated discrete problem. A set of visibility points for each target can then be used as input to a proposed algorithm for the problem, and the problem can then be easily stated. We wish to find a minimal distance circuit which passes through one visibility point for each target.

The problem which we have chosen illustrates many of the mathematically interesting parts of the problem while abstracting some of the physical complexities. It also provides a foundation for further research because we can add physical complexity piece by piece. As our model of the real world becomes more accurate, the performance of our algorithm in realistic scenarios can increase. Over the next few months we will continue to refine our model and to explore different aspects of the problem.

Additions to our problem will include, but not be limited to:

1. Critical (must-do) and non-critical targets.
2. Time constraints.
3. Different penalty functions for missed requests (Requests may be given weights, or may be worth less outside of the time constraints).
4. Management of multiple UAV's.
5. Flight dynamics and directional visibility points.
6. Threat points which must be avoided.

7. Fuel consumption constraints and the avoidance of maneuvers.

The simulation software has been modified to produce input for our basic problem. It already includes flight dynamics calculations and simulates a sensor on each UAV. An ideal sensor with a short range has been added for this study. As we add more complexities to our problem, the simulation will provide a measure of how well our algorithm will work in a real scenario.

4.2 A Mathematical Model

Suppose we are given M possible target locations, denoted by T^k for $k = 1, \dots, M$, to view. There is a visibility region, denoted by R^k , from which each target location T^k can be viewed. The visibility region depends on factors including sensor type, terrain, and minimal safe viewing distance. In some way, we choose several key points within each R^k . (See figure 2.1) This discretizes R^k into N^k representative points P_i^k ($i = 1, \dots, N^k$). If we choose the points correctly, we can take target movement and error margins into account. (In our notation, we use superscripts to denote the corresponding target and subscripts to denote the corresponding visibility point within the region.)

Next, we define a cost c_{ij}^{kl} of traveling from point P_i^k in visibility region R^k to point P_j^l in visibility region R^l . This cost may be determined in Euclidean space, or may be calculated based on threat avoidance. (See <http://ndsun.cs.ndsu.nodak.edu/www/ORION> for an example of this type of calculation.) Instead, it may also include energy or fuel consumption. Finally, assume that the UAV is initially located at a position denoted by P_0^0 which is the only point in starting region R^0 .

One might represent this problem using a directed graph $\mathcal{G} = (\mathcal{N}, \mathcal{A})$ where \mathcal{N} denotes the node set and \mathcal{A} , the arcs. Now let \mathcal{A}^{kl} be the arcs that go from region R^k to region R^l . In the current definition, we do not allow arcs to go from a point in a region to another point in the same region, because we only wish to visit one point from each region. Now, define a zero-one variable

$$y_{ij}^{kl} = \begin{cases} 1, & \text{if vehicle travels from } P_i^k \text{ in region } R^k \text{ to point } P_j^l \text{ in region } R^l; \\ 0, & \text{otherwise.} \end{cases} \quad (4.1)$$

This definition also includes the starting point P_0^0 . We formulate the problem as

$$\text{Minimize} \sum_{k=0}^M \sum_{l=1, l \neq k}^M \sum_{(i,j) \in \mathcal{A}^{kl}} c_{ij}^{kl} y_{ij}^{kl} \quad (4.2a)$$

(We wish to minimize the total travel cost)

Subject to:

$$\sum_{l=1}^M \sum_{(0,j) \in \mathcal{A}^{0l}} y_{0j}^{0l} = 1 \quad (k = 0) \quad (4.2b)$$

(The UAV must go from the starting point to a visibility point.)

$$y_{0j}^{0l} \leq \sum_{k=1, k \neq l}^M \sum_{\{i | (j,i) \in \mathcal{A}^{lk}\}} y_{ji}^{lk} \quad \text{for } j = 1, \dots, N^l \text{ and } l = 1, \dots, M \quad (4.2c)$$

(After reaching the first visibility point, the UAV must leave from the same point. This is a continuity constraint. The reason for the inequality is to account for leaving visibility points which were not entered from the start point.)

$$\sum_{k=1, k \neq l}^M \sum_{(i,j) \in \mathcal{A}^{kl}} y_{ij}^{kl} = 1 \quad \text{for } l = 1, \dots, M \quad (4.2d)$$

$$\sum_{l=1, l \neq k}^M \sum_{(i,j) \in \mathcal{A}^{kl}} y_{ij}^{kl} = 1 \quad \text{for } k = 1, \dots, M \quad (4.2e)$$

(The UAV must fly into each visibility region l from exactly one other visibility region, and must fly out of each visibility region k to go to exactly one other visibility region. Combined, these constraints mean that we cycle through all the regions except the starting point.)

$$\sum_{k=1, k \neq l}^M \sum_{\{i | (i,j) \in \mathcal{A}^{kl}\}} y_{ij}^{kl} = \sum_{m=1, m \neq l}^M \sum_{\{n | (j,n) \in \mathcal{A}^{lm}\}} y_{jn}^{lm}$$

for $j = 1, \dots, N^l$ and $l = 1, \dots, M$ (4.2f)

(If we go to one point in a region, we must leave the same point. This ensures that all cycles are connected, and is a continuity constraint. Note that the arc from the starting point is a special case which is included in 4.2c and is therefore not included in this constraint.)

$$\sum_{k \in Q} \sum_{l \in Q} \sum_{(i,j) \in \mathcal{A}^{kl}} y_{ij}^{kl} \leq |Q| - 1 \quad \text{for all proper subsets } Q \text{ of } \{1, \dots, M\} \quad (4.2g)$$

(This ensures that no cycle includes less than all of the regions. Thus, there is only one cycle, and it is the one we want)

$$y_{ij}^{kl} \in \{0, 1\} \text{ for all } (i, j, k, l) \quad (4.2h)$$

(Either an arc is used or it is not.)

5 Conclusion

Automated decision making can reduce the risk of human error and save lives. Furthermore, machines can make many types of calculations faster than humans, enabling a more capable and efficient military force when used properly. Many problems which have been traditionally solved by human intuition are very difficult to solve computationally. Most of these problems can be classified as NP-hard, which means that the amount of time required to find an optimal solution grows exponentially (unless $P = NP$). The routing problem for surveillance platforms is one example.

Surveillance platforms must fly in a path which allows for visibility of desired targets or regions. As part of our ongoing research effort, we will be implementing Lagrangean relaxation-based methods to this problem. Our results will be shown in a simulation environment based on an unmanned air vehicle. Results approaching optimal with low computational costs are expected, as these methods have performed well on several similar problems. We will continue to refine the problem to include more physical complexities as time goes on.

Thus far, we have posed a visibility based UAV routing problem and given rationale for needing to solve it. We have also developed a mathematical model for this problem. By considering visibility regions, we add a great deal of complexity to the problem, but we may also drastically increase our ability to scan more targets. The initial model will be extended to include multiple UAV's, priorities, time windows, flight dynamics, and several other complexities, such as those found in [1]. At each step along the way, we will test different algorithms to compare performances.

Acknowledgements: I would like to extend thanks to the AFRL/IFEA group for the opportunity to work on this research during the summer. Of special note are Rick Gassner, my lab contact, and Jon Jones, who helped us to fit our problem into the overall OBATS scenario and provided ideas for future work. Also, I would like to thank Jeff Brandtstat and Paul Redmond for their help with the UAV simulation software.

References

- [1] L. D. Bodin, F. L. Golden, A. A. Assad, and M. O. Ball, *Routing and scheduling of vehicles and crews: The state of the art*, Computers and Operations Research **10** (1983), 69–211.
- [2] Booz, Allen, and Hamilton, *Obats resource allocation requirements*, Tech. report, Booz, Allen and Hamilton , INC., 1997.
- [3] T. L. Magnanti, *Combinatorial optimization and vehicle fleet planning: Perspectives and prospects*, Networks **11** (1981), 179–214.
- [4] Abraham Silberschatz and Peter Baer Galvin, *Operating systems concepts*, Addison-Wesley Pub Co, 1997.

Kevin Crossway's report was not available at the time of publication.

EMPIRICAL AND THEORETICAL FOUNDATIONS FOR A
TWO-DIMENSIONAL NON-HOMOGENEITY DETECTOR
FOR RADAR

Brian R. Waterhouse
Graduate Student
Department of Mathematics

Syracuse University
215 Carnegie Library
Syracuse, NY 13210

Final Report for:
Graduate Student Research Program
Air Force Research Laboratory
Sensors Directorate

Sponsored by:
Air Force Office of Scientific Research
Bolling Air Force Base, DC

and

Air Force Research Laboratory
Sensors Directorate

August 1998

EMPIRICAL AND THEORETICAL FOUNDATIONS FOR A
TWO-DIMENSIONAL NON-HOMOGENEITY DETECTOR
FOR THE RADAR PROBLEM

Brian R. Waterhouse
Graduate Student
Department of Mathematics
Syracuse University

Abstract

We are interested in target detection and the radar problem. We looked at i.i.d. data generated by MATLAB and developed a nonparametric test statistic to test for homogeneity in two dimensions. Additional MATLAB programs were written to facilitate this analysis and a method was shown to develop tables for the statistic.

EMPIRICAL AND THEORETICAL FOUNDATIONS FOR A
TWO-DIMENSIONAL NON-HOMOGENEITY DETECTOR
FOR THE RADAR PROBLEM

Brian R. Waterhouse

Introduction

There is a great need for automatic detection processing in engineering applications, particularly in RADAR and SONAR. Although there is much on the study of this problem in one dimension in the literature, little work has been done in the development of higher dimensional models. In this paper, the author attempts to generate more interest in this problem by using visualization tools and computer programs to develop a numerical statistic. (See **Appendix A** for program descriptions.)

Methodology

Suppose that we are given a $N \times M$ test matrix $X = \{x_{ij}\}$ where the i and j are counting variables related to "some" distinguishing features such as range and cross range (angle) in the radar problem ($i = 1, \dots, N$ and $j = 1, \dots, M$). Then each x_{ij} corresponds to a range cell in radar. We wish to find a statistic to test the null hypothesis that the environment is homogeneous; that is, we wish to determine if the range and angle data have the same underlying probability distribution function. One way to consider this problem is to compare the relative percentile data in range with the relative percentile data in cross range and determine if they are "close."

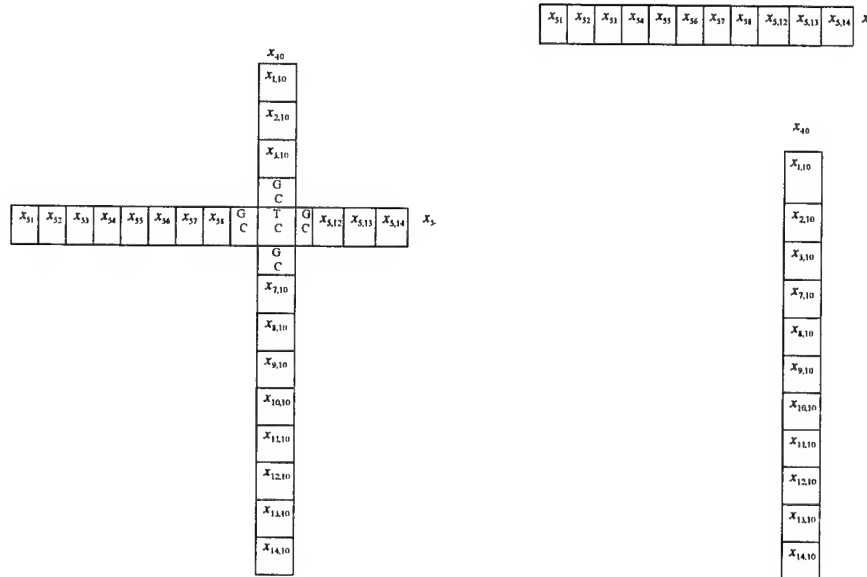
Suppose that we are interested in the test cell x_{kl} as a range cell that possibly has a target. To avoid error we exclude this test cell and the so-called guard cells from our analysis. The *guard cells* are defined to be the range cells adjacent to the test cell (in this case $x_{k-1,l}$, $x_{k+1,l}$, $x_{k,l+1}$, and $x_{k,l-1}$). Thus we do our analysis on $N + M - 6$ cells. For convenience of notation we will continue to use x_k to denote the k th row after exclusion of the test and guard cells and x_l to denote the l th column after the exclusion of the test and guard cells. We will call x_k the *range vector* and x_l the *angle vector*. Let [i] denote the i th entry after ordering. (See **Figure 1**.)

Figure 1. Example of a Scenario

X is 14 X 14

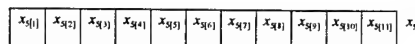
$x_{5,10} = T$ C = target cell

G C = guard cell

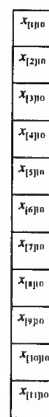


(a) Set up of the Scenario

(b) Deletion of Guard and Target Cells



x_{10}



(c) Ordering of the Vectors

Let $N = M$. Pick the target cell corresponding to $[k] = [l] = a$, where a is an integer. If the null

hypothesis is true, we expect that $\frac{x_{[i]l}}{x_{k[j]}} = \frac{x_{al}}{x_{ka}} \approx 1$. a corresponds to a certain percentile for both the range

vector and the angle vector. For a given test cell we can examine the behavior of this quotient dependent upon the percentiles. We will call the graph of this quotient as a function of the percentile a *percentile plot* for the given test cell. Unfortunately, an analysis along these percentiles shows us that this statistic is not well behaved around the around the 50th percentiles. This is due to the fact that we are assuming that our

distributions have mean 0. Thus if we think of $\frac{x_{al}}{x_{ka}}$ as a function of percentile, at the fiftieth percentile

both $x_{ka} \approx 0$ and $x_{al} \approx 0$. So $\frac{x_{al}}{x_{ka}}$ is not well behaved around this percentile. (see **Figure 2**).

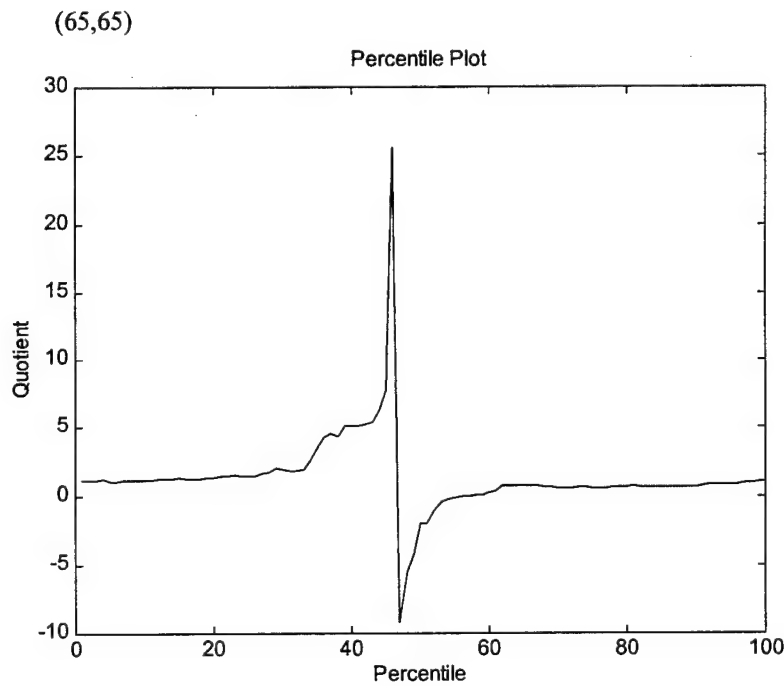


Figure 2. The Percentile Plot for a Gaussian 100×100 test matrix with mean 0 and unperturbed variance 3 with test cell (65,65).

Furthermore, if we assume that the underlying distribution function is Gaussian, it can be shown

theoretically that $\frac{x_{al}}{x_{ka}}$ is not well behaved at higher and lower percentiles, since at the extreme percentiles

the variability of our realization is much greater than at the middle percentiles. Even if we do not assume that the underlying distribution is Gaussian, we may still run into trouble due to the aforementioned ill behavior. (See **Figure 3.** below) So our first guess at an indicator turns out to not be a very reliable one.

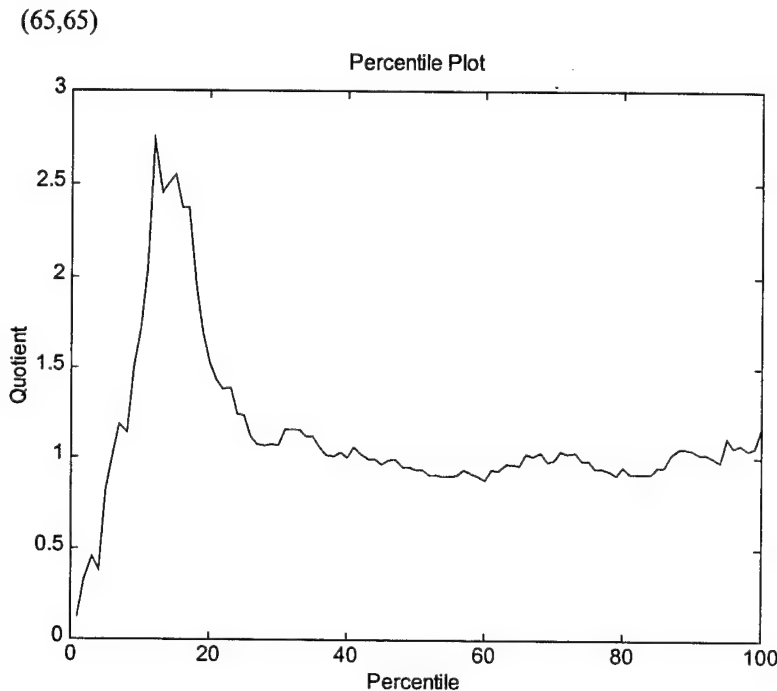
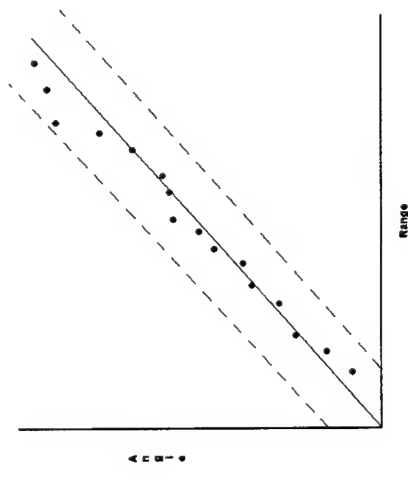


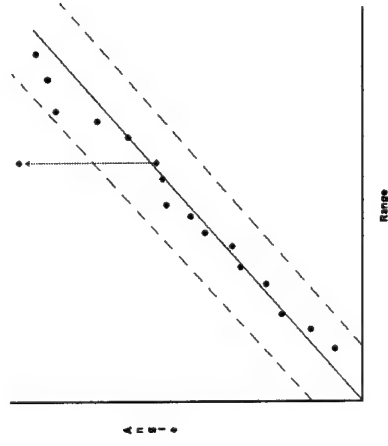
Figure 3. The Percentile Plot for a 100×100 test matrix with a Rayleigh distribution, mean 0, and unperturbed variance 3 with test cell (65,65).

It turns out that a good way to think about this problem is to look at a modified QQ-plot. For a given point (target cell) we take the corresponding row (range) vector and column (angle) vector of our test matrix X and plot ranked row values versus ranked column values. If the data are i.i.d., we expect a 45° straight line to be the best least squares fit to the data. If we can somehow come up with error bars around our 45° straight line, we can then test for homogeneity. (See **Figure 4.**)

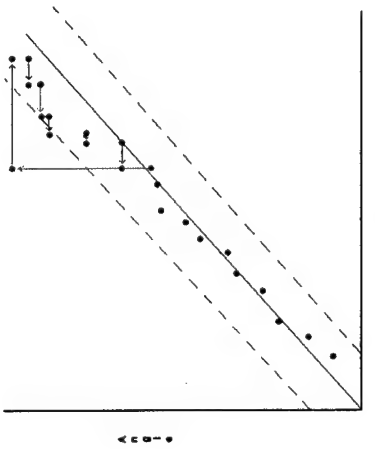
Figure 4. Rationale for the QQ-like plot.



(a) QQ-like plot for i.i.d. data with error bars



(b) A target is introduced into a range cell,
causing that range percentile to correspond to
a higher angle percentile.



(c) As a result, range percentiles are shifted
left possibly outside of the error bars

If we consider our best fit line to be $y = x$, we can use the method of least squares approach from regression to get a measure of the variation the data has from our expected values. So we look at

$s = \sqrt{\frac{1}{n} \sum_{i=1}^n (y_i - x_i)^2}$ where $n = \min(\min(N, M), \min(N, 100))$ and y_i is the angle realization, x_i is the range realization. If we take the mean of many different test cells within the scenario, we should have a pretty good measure of "how" homogeneous the underlying components (range and angle) of the environment are. Now there are some problems with this statistic. First, it is dependent on the size of the matrix. Next, given the size of the matrix, an acceptable value of s changes in relationship to the underlying variance and distribution of the environment. A possible way to overcome these shortcomings is to come up with tables.

An example of a way to do this is to generate, say 1000, scenarios of a 20 X 20 test matrix with i.i.d. data with mean 0 and variance 3. Then look at every possible test cell and compute s and take the mean of these values. If we then delete the top and bottom 25 entries, we would have a pretty good indication of the bounds of the 95% CI for this scenario. Since in practice we do not know the underlying variance of the scene, we include a 95% confidence interval of the minimum and maximum as a reference. (See Table 1.)

20 × 20 i.i.d. (Normal) Test Matrix

Variance	95% Confidence Intervals (Experimental)		
	Minimum	Median	Maximum
3	(0.4703, 0.8246)	(1.7997, 2.2616)	(3.7322, 5.9344)
5	(0.6072, 1.0653)	(2.3234, 2.9204)	(4.8182, 7.7015)
8	(0.7604, 1.3652)	(2.9393, 3.7266)	(5.9750, 9.7354)
10	(0.8775, 1.5398)	(3.2835, 4.1221)	(6.8362, 10.6677)
12	(0.9406, 1.6503)	(3.5993, 4.5243)	(7.4644, 11.8689)
15	(1.0516, 1.8451)	(4.0242, 5.0583)	(8.3454, 13.2698)
17	(1.1195, 1.9643)	(4.2841, 5.385)	(8.8844, 14.1268)

Table 1.

This table was generated using the `iid_table` command, the code for which is included in **Appendix B**. Notice that the relationship between the bounds for variance 3 and the bounds for variance 12 are as expected.

Conclusion

There is a need for test statistics that do not rely on an understanding of the underlying probability distribution function. This is true not only in radar but also in the hard and soft sciences. It is the author's belief that the above statistical method will be found useful in many areas including physics, chemistry, economics, and sociology; basically any study that involves the comparison of two distinct populations. It is the author's hope that this paper will facilitate the development of tables necessary to make this a truly useful statistic.

The author would like to thank Dr. Michael Wicks, without whom this paper would not have been possible.

Appendix A: Matlab Functions

A

angle_vector

```
function y = angle_vector(i, j, test_matrix)
```

(i,j) is the coordinate of the test cell.
The test_matrix is thought of as the x,y-plane.
The angle vector is the jth column of the test matrix.
angle_vector returns the angle vector with the test cell and
the angle guard cells removed.

D

diff_per_plot

```
function plot = diff_per_plot(D,test_i,test_j)
```

Plots the difference Range(%ile) – Angle(%ile) against %ile for
the range vector and the angle vector associated with the test
cell located at coordinates (test_i,test_j).

diff_plot_test

```
function test = diff_plot_test(D, step_x, step_y, percentile)
```

Takes an nXm test matrix, D, and iteratively finds the range
and angle vectors corresponding to the target cell
located at the coordinates (i,j), where i ranges from 1 to n
by step_x and j ranges from 1 to m by step_y. From these
it computes the mean and variance in both the range
and angle vectors. It then locates the
(percentile * range_size)th range cell and
(percentile * angle_size)th angle cell and computes the
difference of these two, each normalized by their standard
deviations. It then plots i vs. j vs. this difference.

diff_test

```
function test = diff_test(D, target_i, target_j, percentile)
```

Takes an nXm test matrix, D, and finds the range
and angle vectors corresponding to the target cell
located at the coordinates (target_i,target_j). From these
it computes the mean and variance in both the range
and angle vectors. It then locates the
(percentile * range_size)th range cell and
(percentile * angle_size)th angle cell and computes the
difference of these two, each normalized by their standard
deviations.

I

iid_table

```
function iid_table = iid_table(n, m, var, number)
```

Creates 'number' test matrices which are $n \times m$ with mean 0, variance 'var', and no x or y trend. It returns a 'number' X 4 matrix where the first column is the minimum of the st dev statistic for the test matrix associated with the row number, the second column is the mean of the st dev statistic for the test matrix associated with the row number, the third column is the maximum of the st dev statistic for the test matrix associated with the row number, and the fourth column is the standard deviation of the the st dev statistics for the test matrix associated with the row number.

M

mean_est

```
function u = mean_est(trimmed_vector)
```

Estimates the mean of the target cell by taking the mean of the "representative" cells.

N

n

```
function y = N(mu, sigma_2)
```

Realizes a random number from a normal curve with mean 'mu' and variance 'sigma_2'

P

percentile_plot

```
function plot = percentile_plot(D,test_i,test_j)
```

Plots the ratio Range(%ile)/Angle(%ile) against %ile for the range vector and the angle vector associated with the test cell located at coordinates (test_i,test_j). Range(%ile) and Angle(%ile) have been normalized by their standard deviations.

percentile_plot2

```
function plot = percentile_plot2(D,test_i,test_j)
```

Plots the ratio Range(%ile)/Angle(%ile) against %ile for the range vector and the angle vector associated with the test cell located at coordinates (test_i,test_j). Range(%ile) and Angle(%ile) have not been normalized by their standard deviations.

percentile_plot_abs

```
function plot = percentile_plot_abs(D,test_i,test_j)
```

Plots the ratio |Range(%ile)/Angle(%ile)| against %ile for the range vector and the angle vector associated with the test cell located at coordinates (test_i,test_j). Range(%ile) and Angle(%ile) have been normalized by their standard deviations.

perturb

```
per = perturb(D, percent, magnitude)
```

If D is an nXm matrix, perturb creates another nXm matrix consisting mostly of zeros. There are 'percent'*n*m/100 nonzero entries located randomly within the matrix. These nonzero entries consist of the realization of a normal distribution * 'magnitude'.

perturbed_qqish_plot

```
function plot = perturbed_qqish_plot(D, target_i, target_j, per, mag)
```

Creates a plot of the percentiles of the range vector vs. the percentiles of the angle vector for the target cell located at the coordinates (target_i,target_j) of the test matrix D. It plots these points in red as +'s and plots the function y = x (the expected relationship between the two variables). It plots the error bars in green. It then perturbs D by 'per %' with magnitude 'mag' and plots the percentiles of the range vector vs. the percentiles of the angle vector for the target cell located at the coordinates (target_i,target_j) of the perturbed matrix. It plots these points in blue as o's.

Q

qqish_plot

```
function plot = qqish_plot(D, target_i, target_j)
```

Creates a plot of the percentiles of the range vector vs. the percentiles of the angle vector for the target cell located at the coordinates (target_i,target_j) of the test matrix D. It plots these points in blue as o's and plots the function y = x (the expected relationship between the two variables.) It then runs a regression on this plot and returns the slope as b.

qqish_plot2

```
function plot = qqish_plot2(D, target_i, target_j)
```

Creates a plot of the percentiles of the range vector vs. the percentiles of the angle vector for the target cell located at the coordinates (target_i,target_j) of the test matrix D. It plots these points in red as '+'s and plots the function $y = x$ (the expected relationship between the two variables.) It then plots the error bars in green.

R

range_vector

```
function y = range_vector(i, j, test_matrix)
```

(i,j) is the coordinate of the test cell.
The test_matrix is thought of as the x,y-plane.
Returns the range vector with the test cell and
the range guard cells removed.

ratio_plot_test

```
function test = ratio_plot_test(D, step_x, step_y, percentile)
```

Takes an nXm test matrix, D, and iteratively finds the range and angle vectors corresponding to the target cell located at the coordinates (i,j), where i ranges from 1 to n by step_x and j ranges from 1 to m by step_y. From these it computes the mean and variance in both the range and angle vectors. It then locates the ('percentile' * range_size)th range cell and ('percentile' * angle_size)th angle cell and computes the ratio of the range cell over the angle cell, each normalized by their standard deviations. It then plots i vs. j vs. this ratio.

ratio_test

```
function test = ratio_test(D, target_i, target_j, percentile)
```

Takes an nXm test matrix, D, and finds the range and angle vectors corresponding to the target cell located at the coordinates (target_i,target_j). From these it computes the mean and variance in both the range and angle vectors. It then locates the ('percentile' * range_size)th range cell and ('percentile' * angle_size)th angle cell and computes the quotient of these two, each normalized by their standard deviations.

ratio_test_2

```
function test = ratio_test_2(D, target_i, target_j, percentile)
```

Takes an nXm test matrix, D, and finds the range and angle vectors corresponding to the target cell located at the coordinates (target_i,target_j). From these it computes the mean and variance in both the range and angle vectors. It then locates the ('percentile' * range_size)th range cell and ('percentile' * angle_size)th angle cell and computes the quotient of these two, without normalization by their standard deviations.

S

sdev_stat_gen

```
function plot = sdev_stat_gen(D)
```

If D is an mXn matrix, sdev_stat_gen returns an mXn matrix with the entry (i,j) consisting of the standard deviation of the qqish plot of the target cell located at coordinates (i,j) with regards to the line $y = x$. (We are looking at the square root of the sum of the squares of the differences between the Range(%ile) and the Angle(%ile) divided by max(m,n).)

sig_i_sq

```
function y = sigma_i_sq(sigma_i_0_sq, sigma_i_x_sq, sigma_i_y_sq, x, y)
```

Calculates the variance of the ith component of the target cell.

'sigma_i_0_sq' is a fixed number representing the underlying variance.
'sigma_i_x_sq' is a fixed number representing the trend of the variance in the x (range) direction.
'sigma_i_y_sq' is a fixed number representing the trend of the variance in the y (angle) direction.
(x,y) are the coordinates of the cell.

sorter

```
function sorter = sorter(matrix_X)
```

sorter takes 'matrix_X' and sorts its rows and columns.

sum_stat_gen

```
function y = sum_stat_gen(D)
```

If D is an mXn matrix, sum_stat_gen returns an mXn matrix with the entry (i,j) consisting of the sum of squares of the differences between the Range(%ile) and the Angle(%ile) for the target cell located at coordinates (i,j).

T

test_data

```
function test_data = test_data(n, m, mu, sigma_i_0_sq, sigma_i_x_sq, sigma_i_y_sq)
```

Returns an n X m matrix that represents normal data in the field.
sig_i_0_sq, sig_i_x_sq, and sig_i_y_sq are constants used to
determine the variance of the test data.

test_data_abs

```
function test_data = test_data(n, m, mu, sigma_i_0_sq, sigma_i_x_sq, sigma_i_y_sq)
```

Returns an n X m matrix that represents rayleigh data in the field.
sig_i_0_sq, sig_i_x_sq, and sig_i_y_sq are constants used to
determine the variance of the test data

V

var_est

```
function s_2 = var_est(trimmed_vector)
```

Estimates the variance of the target cell using
the MLE of the "representative" cells.

Appendix B: Code for iid_table

There are six functions that are needed in order to run iid_table: N, sig_i_sq, test_data, range_vector, angle_vector, and sdev_stat_gen.

N

```
function y = N(mu, sigma_2)

% function y = N(mu, sigma_2)
%
% Realizes a random number from a normal curve with mean mu
% and variance sigma_2

y = randn*(sigma_2)^.5 + mu;
```

sig_i_sq

```
function sig_i_sq= sig_i_sq(sigma_i_0_sq,sigma_i_x_sq,sigma_i_y_sq,x,y)

% function y = sigma_i_sq(sigma_i_0_sq, sigma_i_x_sq, sigma_i_y_sq,x,y)
%
% Calculates the variance of the ith component of the
% target cell.
%
% sigma_i_0_sq is a fixed number representing the underlying variance.
% sigma_i_x_sq is a fixed number representing the trend of the
% variance in the x (range) direction.
% sigma_i_y_sq is a fixed number representing the trend of the
% variance in the y (angle) direction.
% (x,y) are the coordinates of the cell.
```

```
sig_i_sq = sigma_i_0_sq + x*sigma_i_x_sq + y*sigma_i_y_sq;
```

test_data

```
function test_data = test_data(n, m, mu, sig_i_0_sq, sig_i_x_sq, ...
                                sig_i_y_sq)

% function test_data = test_data(n, m, mu, sigma_i_0_sq, sigma_i_x_sq,
%                                sigma_i_y_sq)
%
% Returns an n X m matrix which represents normal data in the field.
% sig_i_0_sq, sig_i_x_sq, and sig_i_y_sq are constants used to
% determine the variance of the test data

for i = 1:n
    for j = 1:m
        matrix_X(i,j) = N(mu,sig_i_sq(sig_i_0_sq, sig_i_x_sq, ...
                                         sig_i_y_sq, i, j));
    end
end
test_data = matrix_X;
```

range_vector

```
function range_vector = range_vector(i, j, test_matrix)

% function y = range_vector(i, j, test_matrix)
%
% (i,j) is the coordinate of the test cell.
% The test_matrix is thought of as the x,y-plane.
% Returns the range vector with the test cell and
% the range guard cells removed.

[n,m] = size(test_matrix);
y = test_matrix(:,j);
if and(i-2 >= 1, n-3 >= i-1)
    for k = 1:i-2
        r_vector([k]) = y(k);
    end
    for k = i-1:n-3
        r_vector([k]) = y(k+3);
    end
    range_vector = r_vector';
elseif and(i == 1, n-3 >= 1)
    for k = 3:n
        r_vector(k-2) = y(k);
    end
    range_vector = r_vector';
elseif and(i == 2, n-3 >=1)
    for k = 4:n
        r_vector(k-3) = y(k);
    end
    range_vector = r_vector';
elseif and(i == n, n>=3)
    for k = 1:n-2
        r_vector(k) = y(k);
    end
    range_vector = r_vector';
elseif and (i == n-1, n>=4)
    for k = 1:n-3
        r_vector(k) = y(k);
    end
    range_vector = r_vector';
else
    range_vector = 'Bad data - check i and j'
end
```

angle_vector

```
function angle_vector = angle_vector(i , j, test_matrix)

% function y = angle_vector(i, j, test_matrix)
%
% (i,j) is the coordinate of the test cell.
% The test_matrix is thought of as the x,y-plane.
% The angle vector is the jth column of the test matrix.
% angle_vector returns the angle vector with the test cell and
% the angle guard cells removed.

[n,m] = size(test_matrix);
y = test_matrix(i,:);
if and(j-2 >= 1, m-3 >= j-1)
    for k = 1:j-2
        a_vector([k]) = y(k);
    end
    for k = j-1:m-3
        a_vector([k]) = y(k+3);
    end
    angle_vector = a_vector';
elseif and(j == 1, m-3 >= 1)
    for k = 3:m
        a_vector(k-2) = y(k);
    end
    angle_vector = a_vector';
elseif and(j == 2, m-3 >=1)
    for k = 4:m
        a_vector(k-3) = y(k);
    end
    angle_vector = a_vector';
elseif and(j == m,m>=3)
    for k = 1:m-2
        a_vector(k) = y(k);
    end
    angle_vector = a_vector';
elseif and (j == m-1, m>=4)
    for k = 1:m-3
        a_vector(k) = y(k);
    end
    angle_vector = a_vector';
else
    angle_vector = 'Bad data - check i and j'
end
```

stdev_stat_gen

```
function y = sdev_stat_gen(D)

% function plot = sdev_stat_gen(D)
%
% If D is an mXn matrix, sdev_stat_gen returns an mXn matrix with
% the entry (i,j) consisting of the standard deviation of the qqish
% plot of the target cell located at coordinates (i,j) with regards
% to the line y = x. (We are looking at the square root of the sum
% of the squares of the differences between the Range(%ile) and the
% Angle(%ile) divided by max(m,n).)

[m,n] = size(D);
for target_i = 1:m
    for target_j = 1:n
        x = range_vector(target_i,target_j,D);
        y = angle_vector(target_i,target_j,D);
        new_x = sorter(x);
        new_y = sorter(y);
        range_size = size(new_x,1);
        angle_size = size(new_y,1);
        sum = 0;
        for k = 1:100
            range_position = round((k/100)*range_size);
            if range_position == 0
                range_position = 1;
            end
            angle_position = round((k/100)*angle_size);
            if angle_position == 0
                angle_position = 1;
            end
            if range_position < range_size
                if angle_position < angle_size
                    sum = sum+(new_x(range_position)-
new_y(angle_position))^2;
                else
                    sum = sum +(new_x(range_position)-new_y(angle_size))^2;
                end
            else
                if angle_position < angle_size
                    sum = sum +(new_x(range_size)-new_y(angle_position))^2;
                else
                    sum = sum +(new_x(range_size)-new_y(angle_size))^2;
                end
            end
            end
            sum ;
            sample_var = sum/max(range_size,angle_size);
            st_dev(target_i,target_j) = sample_var^.5;
        end
    end
y = st_dev;
```